A RECONFIGURATION ALGORITHM FOR A DC ZONAL ELECTRIC DISTRIBUTION SYSTEM BASED ON GRAPH-THEORY METHODS

By

Julia P. Certuche-Alzate

A thesis submitted in partial fulfillment of the requirements for the degree of

MASTER OF SCIENCE

in

ELECTRICAL ENGINEERING

UNIVERSITY OF PUERTO RICO
MAYAGÜEZ CAMPUS

2009

Approved by:

Efraín O'Neill Carrillo, Ph.D Member, Graduate Committee	Date
Manuel Rodríguez Martínez, Ph.D Member, Graduate Committee	Date
Miguel Vélez Reyes, Ph.D President, Graduate Committee	Date
Ana Carmen González, M.S. Representative of Graduate Studies	Date
Isidoro Couvertier, Ph.D Chairperson of the Department	Date

Abstract of Dissertation Presented to the Graduate School
of the University of Puerto Rico in Partial Fulfillment of the
Requirements for the Degree of Master of Science

A RECONFIGURATION ALGORITHM FOR A DC ZONAL ELECTRIC DISTRIBUTION SYSTEM BASED ON GRAPH-THEORY METHODS

By

Julia P. Certuche-Alzate

May 2009

Chair: Miguel Vélez Reyes
Major Department: Electrical and Computer Engineering

In many applications, self contained Electric Power Distribution Systems (EPDS) require high survivability under fault conditions. A fault produces an immediate change in the system topology resulting in potential loss of energy to critical system components and system collapse.

During fault conditions, it is required for the EPDS to maintain a minimum level of functionality. To achieve this goal, it is necessary to have supervisory control systems that can reconfigure the system topology from a fault condition to a new topology that meets minimal operation requirements.

This thesis presents an reconfiguration algorithm for EPDS, specifically for DC Zonal Electric Distribution Systems (DCZEDS), which solves the reconfiguration problem as a maximum flow optimization problem for power balance under safe operating conditions that takes load priority into consideration and minimizes the switching operations to achieve the new EPDS topology. The main tool is graph-theory, where the reconfiguration problem is solved by solving a multi-objective network flow optimization problem. Simulation results are presented that demonstrate the functionality of the proposed approach.

Resumen de Disertación Presentado a Escuela Graduada
de la Universidad de Puerto Rico como requisito parcial de los
Requerimientos para el grado de Maestría en Ciencias

ALGORITMO DE RECONFIGURACIÓN PARA UN SISTEMA DE DISTRIBUCIÓN ELÉCTRICO ZONAL DC USANDO TEORÍA DE GRAFOS

Por

Julia P. Certuche-Alzate

Mayo 2009

Consejero: Miguel Vélez Reyes
Departamento: Ingeniería Eléctrica y Computadoras

En muchas aplicaciones, la distribución de potencia en sistemas autocontenidos requieren alta estabilidad bajo condiciones de falla. Una falla produce un cambio inmediato en la topología del sistema, ocasionando una potencial pérdida de energía para los sistemas críticos y que el sistema colapse.

Durante condiciones de falla, los sistemas de distribución de potencia requieren mantener un nivel mínimo de funcionalidad. Para alcanzar esta meta, es necesario tener systemas para control supervisorio que puedan reconfigurar la topología del sistema desde una condición de falla hacia una nueva topología que reuna los requerimientos de operacion mínima.

Esta tesis presenta un algoritmo de reconfiguración para sistemas de distribución de potencia autocontenidos, específicamente para sistemas zonales DC (DC ZEDS), el cual resuelve el problema de reconfiguración como un problema de optimización de flujo máximo para balance de potencia bajo condiciones de operación seguras, considerando la prioridad de cargas y minimizando las operaciones de conmutación para alcanzar la nueva topología del sistema. La herramienta utilizada es la teoría de grafos, donde el problema de reconfiguración es resuelto solucionando un problema multiobjetivo de optimización de flujo en redes. Resultados de simulación son presentados para demostrar la funcionalidad del algoritmo propuesto.

A mis mejores auspiciadores de sueños

y maestros de vida

...mis padres.

ACKNOWLEDGMENTS

Thanks to God for giving me the opportunity, looking into the bright side of my life and also for giving me the strength to overcome all obstacles encountered in the course of my studies in University of Puerto Rico, Mayagüez.

This work would not have been possible without the experience, knowledge, suggestions and patience from my advisor, Dr. Miguel Vélez Reyes for whom I am thankful. I am grateful to my thesis committee members, Dr. Efrain O'Neill Carrillo and Dr. Manuel Rodríguez Martínez for their review and helpful criticism.

Special thanks go to my mother, father, sister and brother for their love, support and motivation towards my studies. Also, my appreciation goes to Wilber for his encouragement, advice, support, true friendship towards me, and for be with me all the time. I want to thank to my sister Lili, and my friends Elkin, Fercha, Leidy, Jesu, Carito, Horacio, Paola and Javier, because during my time in Puerto Rico, they always give me their unconditional help, efforts and friendship. I would like to thank my graduate fellows for made my time at UPRM unforgettable.

I am grateful to God for blessing me with my heart desire, Pablo Lozada who has made my time in Puerto Rico enjoyable and fulfilled.

The Center for Power Electronics CPES, and the Electrical and Computer Engineering Department UPRM provided the funding and resources for the development of this research.

TABLE OF CONTENTS

LIST OF TABLES

LIST OF FIGURES

CHAPTER 1
Introduction

1.1 Justification

Modern DC Power Electric Distribution System requires high survivability under failure conditions. In general, the requirements of installed loads are nearly close to the maximum capacity supplied by a generator, and when a fault occurs, this produces an immediate change in the system topology. The loss of power balance in the system can result in equipment damage, harmful operation conditions and in extreme cases may produce the entire system collapse. Therefore, DC Power Electric Distribution Systems require fast reconfiguration capability in order to maintain critical loads working.

The reconfiguration system is part of the control system reconfiguration developed to maintain operating conditions under failure conditions. The control system reconfiguration includes advanced monitoring and control of all sensors and protective devices, a geographical data base, a fault detection technique, and a reconfiguration technique [13]. Protective devices are used in electric power systems to prevent or limit damage during abnormalities and to minimize their effect on the remainder of the system [13]. The Figure 1–1 shows a basic control system reconfiguration in electric power distribution systems (EPDS), which can be applied centralized or distributed.

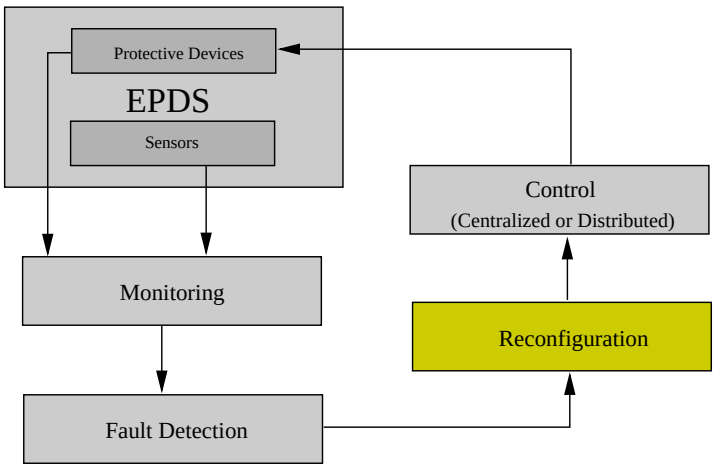

Figure 1–1: Block diagram of the control reconfiguration system for EPDS.

The purpose of power system reconfiguration is to isolate the part of the system where the fault occurred, carrying out a network topology change, and a load shedding scheme to adjust the load demand to the available generation. Moreover, the reconfiguration mechanism looks for the new network configuration that minimizes or maximizes particular system characteristic.

There are many works in power network reconfiguration, most of them take into consideration; fault isolation, load shedding and operational limits. However, the area of DC Power Electric Distribution Systems regarding variable load, and operation system constraints remain open. This research presents an algorithm for network reconfiguration on a DC Zonal Electric Distribution System (DCZEDS), that maximizes the amount of load served, taking into account load shedding, system constraints, loads priority and variable load.

In this research, the graph theory was selected to develop the reconfiguration algorithm, because is very general and has been used in several applications of power system networks, including representation, analysis and simulation. Also, this theory may simplify the representation of switching procedures into a complex

power system. Several power system operations and management problems can be formulated as optimization over graphs than can be solved by matrix manipulations.

1.2 Objectives

The main objective of this research is to study a self-reconfiguration of an Electric Power Distribution Systems using methods based on graph theory.

Specific objectives of these work are:

- To study the fundamental concepts of graph theory and its applications in power networks.
- To represent a DC Zonal Electric Distribution System (DCZEDS) using graph theory.
- To design a reconfiguration network algorithm using graph theory.
- To evaluate the algorithm applicability on a DCZEDS under some fault scenarios.
- To evaluate the applicability of the reconfiguration algorithm on different DCZEDS.

1.3 Summary of contributions

The major contributions of this thesis can be summarized as follows:

1. The reconfiguration algorithm is adaptable to any DC zonal system because it is only necessary to define the matrices required by the algorithm; the most important issue is to define the nodes and edges of the system. Therefore for other systems, it is not necessary to change any function or routine into the algorithm to develop the reconfiguration process.
2. Develop of operations over the graph matrices, in order to represent the power network topology changes, and to facilitate seek of the better paths to reconfigure the system.

3. The algorithm takes in consideration the reconfiguration of DC Zonal Electric Distribution Systems for variable loads, and were developed different schemes of load shedding.
4. As it is known, it is possible to generate subsequent fault when the reconfiguration process is done, e.g., if a power constraint is not considered at the moment of selecting a particular node, this decision may results in a new fault. This algorithm has been designed considering power system constraints to avoid these types of faults.

1.4 Thesis Outline

Chapter 2 contains the background theory. Chapter 3 presents a detailed mathematical formulation of the reconfiguration problem as an optimization problem and its application to a DC Zonal Electric Distribution System. Chapter 4 provides a complete description of the reconfiguration algorithm developed. Chapter 5 presents simulation results under some fault scenarios. Finally, Chapter 6 presents conclusions and recommendation for future work.

CHAPTER 2
Literature Review

2.1 Overview

This Chapter presents the basic concepts of Electrical Power Systems, reconfiguration for power system, Graph theory, and a brief comparison between Radial and Zonal configuration. Also describes some reconfiguration process using graph-theory.

2.2 Electric Power Systems

Power systems are one of the most fundamental aspects of electrical engineering, because such systems generate and control the energy that enables all electric and electronic capabilities in the society [1]. Utility Electric Power System (EPS) consists of generation resources, transmission systems, distribution systems, and control [15]. The transmission system interconnects all major generating stations and main load centers in the system. In forms the backbone of the power system and operates at the highest voltage levels (typically, $230KV$ and above). The generator voltages are usually in the range of 11 to $35KV$. These are stepped up to the transmission voltage level, and power is transmitted to transmission substations where the voltages are stepped down to the subtransmission level (typically, $69KV$ to $138KV$). The subtransmission system transmits power in smaller quantities from

the transmission substations to the distribution substations. The distribution system represents the final stage in the transfer of power to the individual customers. The primary distribution voltage is typically between $4.0KV$ and $34.5KV$ [36].

The need for improvement in comfort, convenience, entertainment, safety, communications, maintainability, supportability, survivability, and operating costs require more electric vehicular systems. Therefore, EPS with larger capacities and more complex configurations are required to facilitate increasing electrical demands in advanced vehicles [1]. EPS is an example of a self contained power system such as those implemented into marine, automotive and aerospace applications. These systems have unique system architectures, characteristics, dynamics and stability problems that are not similar to those of utility electrical power systems.

The Electric Power System used in this study is a self-contained shipboard power system. The naval electrical power system attempts to optimize the delivery of electric power to vital loads when faults occurs, due to component failures, load dynamics and hostile disruptions [3].

2.3 Electrical Distribution System in Shipboard

The naval ship power system consists of two main designs namely; segregated and integrated power system. In the segregated power system (SPS), each of the ship services and the ship propulsion load are provided from segregated sets of generators. On the other hand, in the integrated power system (IPS), the ship service and the propulsion loads are provided by a common set of generators [32]. The Naval ship integrated power system consists of AC generators over ground cables,

propulsion loads, inverters, rectifiers and AC-DC ship service loads [1]. The ship power distribution system architecture is designed in various forms based on specific load requirements; radial distribution system, ring distribution system, and zonal distribution system.

2.3.1 Radial Electric Power Distribution system

Today, AC radial or ring-type distribution systems are implemented in shipboard. These systems have multiple generators (typically three or four), which are connected to a number of switchboard panels and the 450V, 60Hz three-phase AC is then distributed throughout the ship to load centers [17].

These systems generate and distribute electric power using an ungrounded delta configuration, allowing the power system operating continuously in the event of a single-phase-to-hull fault [6]. However, this electrical distribution system is expensive due to the high cost of power cables and switchboard feeder circuits [17].

Since the advancement in power electronics, in terms of increase in power density, reliability of power switching, elements with reduced cost, and the advance in control techniques using power electronics converter, different organizations have started looking for new options to change the architecture of electrical power distribution system [1].

2.3.2 Zonal Electric Power Distribution system

In 1997, the ship USS Oscar Austin (DDG 79) was retrofitted from a radial topology to a zonal topology [3]. The radial distribution architecture is contrasted with a zonal approach in Figure 2–1 [52].

In zonal electric distribution system, the conventional shipboard and conventional panels had been replaced with individual power electronics modules installed

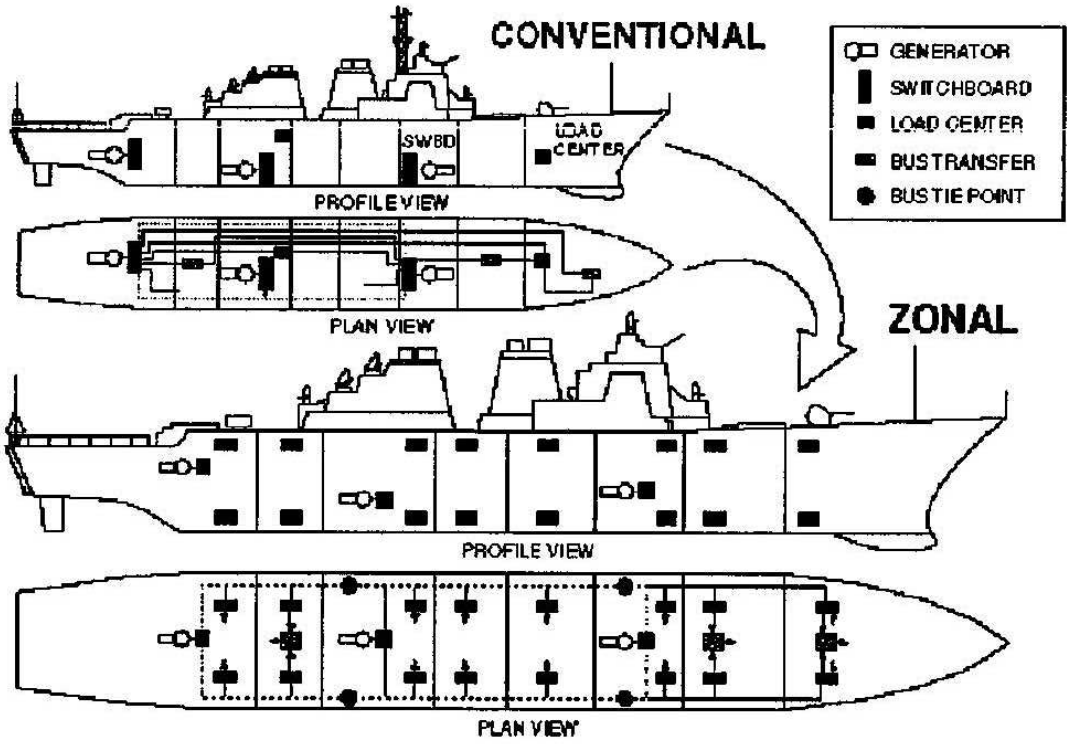

Figure 2–1: Conventional and Zonal Distribution Architectures [52]

on a power bus in the vicinity of respective loads [1]. Furthermore, the power in this topology is provided to loads using longitudinal feeders around the ship, this maximizes the distance between the busses and, in turn, maximizes the survivability of one of the busses during a casualty[3]. Additionally, the effects of damage to the distributed system and other equipment will not disturb generators [52].

For a better understanding of zonal topology, the author in [20] defines a number of key terms, detailed a number of different zonal architectures, described the situations where the architectures are best suited and proposed a framework for zonal ship design.

Zonal distribution architectures provide maximum protection (fault tolerance), reduce cabling, and are cheaper than radial distribution [21]. A zonal distribution

system also allows equipment installation and testing prior to zone assembly [17]. On the other hand, this accomplishes fast reconfiguration of the vital ship systems in the event of fault or when new equipment is introduced. The main bus in Zonal Electric Distribution System ZEDS could be AC or DC.

AC Zonal Electric Distribution System

The AC zonal system employs a new phase-oriented controller that ensures uninterrupted power to critical loads even despite the loss of portions of the power distribution network. This system is suitable for use in either military or commercial (premium power parks) applications, and will yield high power quality in a survivable AC zonal system [21].

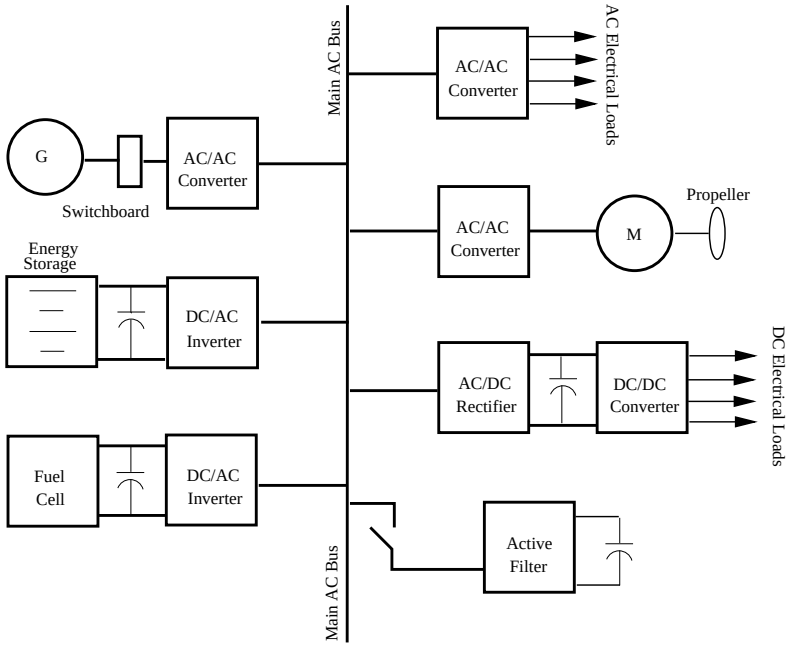

Figure 2–2: AC Zonal Electric Distribution System [1]

An example of an AC zonal distribution is shown in Figure 2–2, where, AC electrical loads receive power from the AC/AC converters at various voltages and

frequencies. AC/AC converters are also used as electric drives for single and three-phase AC motors [21]. Different DC electrical loads in the system receive supply from single or three-phase controlled AC/DC rectifiers. Power quality can be maintained in AC zonal distribution system with active filters for harmonic elimination [1]. However, this type of distribution system has problems of voltage dips at various points in the system due to the transients resulting from any casualty, switching, or sudden increase in power demand [33]. Moreover, variation of voltage and frequency propagates its effect on the entire system, affecting performance of individual equipment and instruments as well as power electronics converters. Therefore, AC zonal electrical distribution systems are unable to meet all distinct features of power electronic based systems.

DC Zonal Electric Distribution System

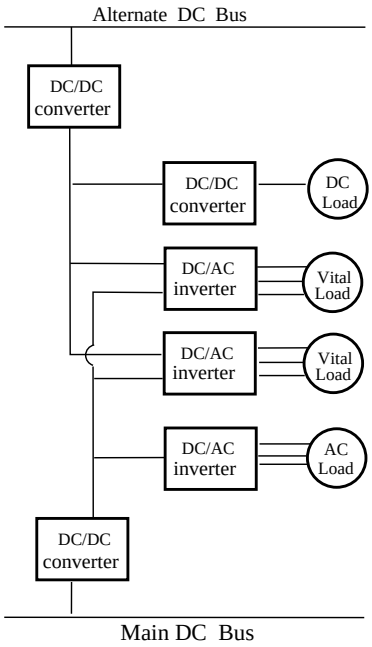

Figure 2–3: DC Zonal Architecture (DCZEDS) [17]

An example of a DC zonal distribution is shown in Figure 2–3. In this type of distribution system, the generator voltages are rectified and the resulting DC

is distributed along the main and alternate busses. Each bus is connected to an electrical zone through a power converter that serves to buffer the main bus and the intra-zone electrical loads [8]. The inverters would then provide the single and three-phase power requirements of the zone. The input buffering converter is a step-down DC/DC buck converter and is termed the Ship Service Converter Module (SSCM) while the DC/AC pulse width modulation (PWM) inverter unit is termed the Ship Service Inverter Module (SSIM)[17].

These power conversion and distribution modules (SSCM's and SSIM's) are multifunctional, performing the power conversion, monitoring and limiting the current through the semiconductor devices and protecting the system during fault conditions [17]. Thus, DCZEDS facilitates isolating faults to an electrical zone and prevent propagation of the fault.

DCZEDS will also offers advantages in terms of the number of power conversion stages. For instance, various combat systems require 400Hz in combination with a number of DC voltages. In the AC distribution system, this would require that the distributed three-phase AC must be rectified, converted to 400Hz with an inverter, shifted to an appropriate voltage level with a transformer, then once again rectified to provide the required DC power. In DCZEDS, there is no need to have an intermediate 60Hz step [17]. Also, the implementation of DCZEDS has reduced the requirement of large AC swithgear and magnetic components, which reduces the size,weight and cost of the overall system [1]. Detection and restoration of faults also become simple because of DC load flow analysis. Furthermore, in this type of distribution system, transients can be restricted to particular zones only with superior control techniques used for individual modules. As the required power conversion for electrical loads is made at separate zones, harmonic distortion is lower than in AC distribution systems and the effects of voltage and frequency variations

are limited [1].

For a distributed system, zonal survivability is the ability of the distributed system, when experiencing internal faults confined to adjacent zones, to ensure loads in undamaged zones do not experience a service interruption. Zonal survivability assures faults do not propagate outside the adjacent zones in which the fault is experienced. For many distributed system design, zonal survivability requires that at least one longitudinal bus remains serviceable, even through damaged zones [20].

2.4 Reconfiguration of Power Systems

In many critical applications, DC Electric Power Distribution Systems require high survivability under failure conditions. In general, the requirements of installed loads are nearly close to the maximum capacity supplied by a generator, and when a fault occurs produces an immediate change in the system topology. Therefore, EPDS require fast reconfiguration in order to maintain critical loads working. Network reconfiguration is mainly done for load restoration, loss minimization, and load balancing [48].

Most of the works have been developed considering a centralized control; these involve expert systems, evolutionary algorithms, artificial intelligence and fuzzy logic [50]. In [61], the author proposed an expert-system-based reconfiguration methodology for load restoration in shipboard power systems.

Other field related with the shipboard reconfiguration, which calls researchers attention is distributed control. Distributed controllers implemented using agents, exchange information to achieve a collective goal [48]. A self-reconfigurable DC Zonal Electric Distribution System (DCZEDS) was developed in order to maximize

the number of served loads with highest priority using MultiAgent Systems (MAS) in [29]. Also, this MAS was capable to respond when a fault is cleared, allowing the system to restore power to loads that were disconnected to supply power to higher priority loads. When there is more than one alternative to feed a load, the MAS connects its loads to the lowest cost option. In this work, the authors assume that load priorities are fixed regardless of changing situations.

The methods agent-based are only interesting with regards to the specified network structure or tasks [48]. Even more general agent-based control schemes are currently lacking in rigorous proof of optimality, especially in severe failure scenarios.

The global concept of the reconfiguration process in this research, is developed thinking in a centralized control, and is based on the adaptive protection algorithm developed by [2], which consists mainly of four main algorithms. These algorithms and their interaction are depicted in the block diagram of Figure 2–4.

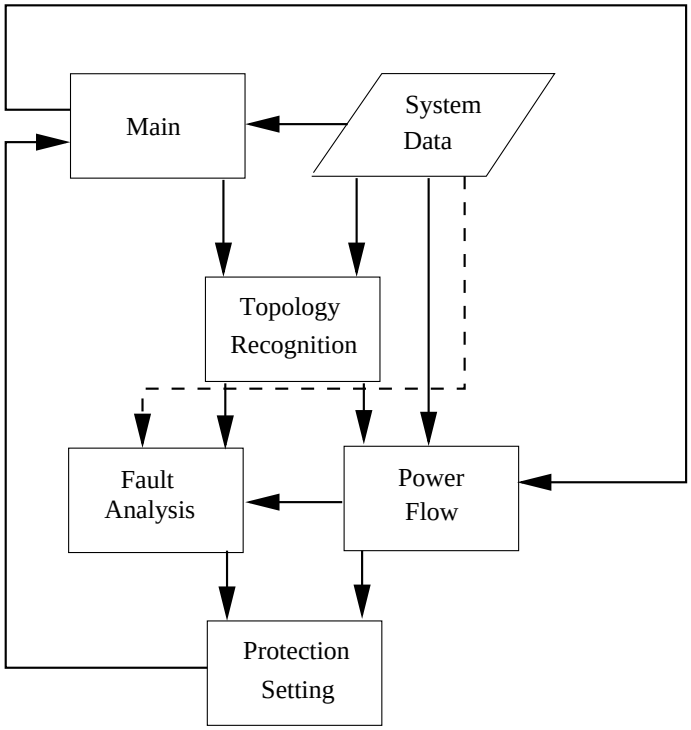

Figure 2–4: Block diagram of the reconfiguration process for EPDS [2]

The reconfiguration process is activated by a signal and can run repeatedly at a specified interval of time. The system data block contains the information and current data of the system to be processed by the four algorithms. These data are received from data sensors, which continually monitor the system parameters and are usually changed by protection and reconfiguration actions. The topology recognition algorithm is used to determine the system configuration from the system data. The Fault analysis algorithm determines the kind of fault occurred and isolates the fault if it is necessary. The power-flow algorithm analyzes the power flow into the system and obtains the optimum power that must to flow through the edges. The protection section algorithm adjusts system protection settings to guarantee an adequate level of protection. These algorithms must be customized according to system because protection setting requires a detailed knowledge of the apparatus to be protected, such as generators, transformers and motors [2].

Some other research directions in network reconfiguration methods have been explored. For example, in [31], the authors worked on loss minimization and fix load balancing for an AC shipboard power system, they proposed a fast reconfiguration algorithm to maintain power balance of the remaining power system parts after fault detection and isolation. They represented the shipboard power system topology using a graph, found the fault location and its impact based on the differential zone protection scheme, and implemented reconfiguration actions to minimize the loss of load considering load priorities without consideration to system constraints.

Graph theory applications in power networks simplify the representation of switching procedures in a complex power system; converting various problems of power system analysis into graph-based problems, and developing system operations through graph-based numerical problems. Also, graph theory can simplify

power system representation and represent any system topology change as a graph operation. Since a shipboard power system is small in area and has possible full system measurement, graph representation of the system topology is helpful in analyzing system reconfiguration and operations [31].

The authors in [31] represented the shipboard power system model showed in Figure 2–5 with a graph. In this model, the main components include service switchboards, buses, cables, generators, and load feeders. Interconnections of these components consist of breakers, circuit transformers (CTs), or combinations of circuit breaker and transformer. The authors show the relationship between the major components of shipboard power system and the corresponding graphical elements in Table 2–1.

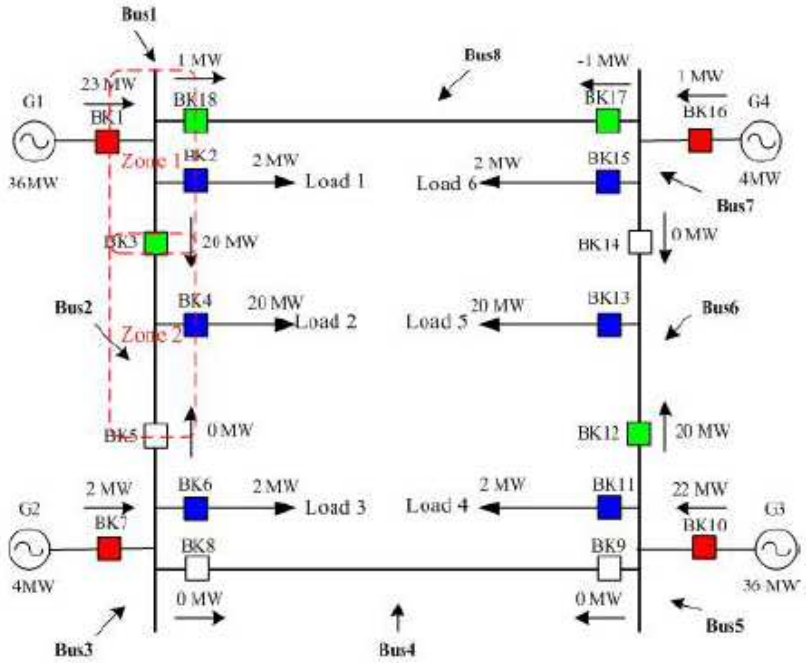

Figure 2–5: A shipboard power system model [31]

Figure 2–6 shows the graph representation of the power system in Figure 2–5. The direction of the edge is related to the polarity of the corresponding CT connection.

Table 2–1: Graph Representation [31]

Components in Shipboard Power Systems	Graph Elements
Service switchboard	Vertex
Bus	Vertex
Cable	Vertex
Generator	Vertex
Load feeder	Vertex
Breaker	Edge
CT	Edge
Breaker-CT	Edge

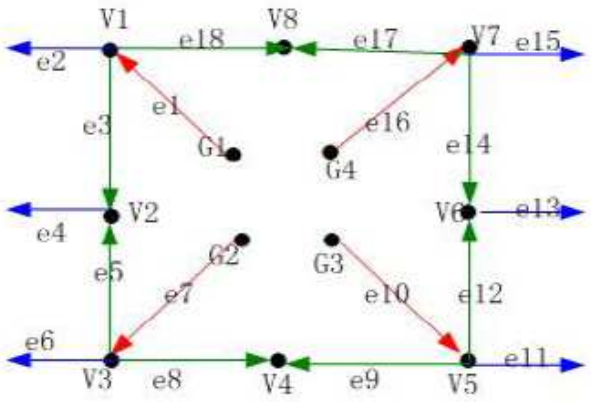

Figure 2–6: Graph representation of the model in Figure 2–5 [31].

They defined that each vertex with its directed edges represents a protection zone. They represent the relationship between nodes and edges, into a matrix named Node-Arc Incidence matrix, for computer implementation. The authors defined other matrices in order to develop the fast reconfiguration algorithm such as: the breaker status matrix represents the system breaker open/close status (BRK_STATUS), the generator capacity contains the index of the generator breaker and the corresponding generator capacity (GEN_CAPACITY), the instantaneous

power flow matrix through each breaker (BRK_FLOW) and the load priority matrix (LOAD_PRIORITY). When single or multiple faults happen on the shipboard power system, the fault detection function will quickly identify the faulted zone(s) and isolate them. The corresponding tripped breaker status in the BRK_STATUS matrix will be updated to zero. Then a new system incidence matrix will be updated after fault isolation by removing the row(s) of the isolated zone(s) and the column(s) of the tripped breaker(s) for fault isolation. The algorithm will stop when it finds a path with non-negative power balance, as well as when the tree space is completely searched [31].

Other works had been developed using graph theory, in [16], a directed graph is used to represent a power system network for power flow and determine the specific generator contributions to different loads. Also an application of graph theory to protection zone selection in microprocessor-based bus relays was done in [53]. They illustrated the graphical representation of station bus arrangements, described graph operations and associated matrix operations for zone selection, and showed an implementation of the zone selection method in microprocessor-based bus relays. A Network with fixed loads was worked by [10], using CPLEX optimization package, they restore a maximum amount of load while satisfying the capacity and voltage constraints directly. The proposed method does not require any load flow/power flow analysis to verify the current and voltage constraints.

Some reconfiguration algorithms may reach unacceptable topologies and some loads have to be shed to reach an acceptable topology. In such situations, algorithms are needed to decide which particular loads will be shed, so that service disruptions are reduced without sacrificing the service quality of critical loads. There are just a few algorithms available to solve this problem, even though load shedding algorithms

are required in several situations. In [57], a simple and effective algorithm has been developed to determine the loads to be shed in order to overcome the abnormal operating conditions in the radial system.

The works referenced before have developed reconfiguration network algorithms with a fixed load scheme, but the truth is that; the load demand is varying continuously (e.g. variable-speed AC motor controller).

In [47], the discussion of static problems (ignoring all transient effects) focused on performance improvement through minimization of network losses and prevention of distribution cable overloads. The authors minimized losses through an optimal allocation of discretionary currents in a managed network (DC networks), [45], or through reconfiguration of the network topology [46].
That work considered a distribution network having N nodes, each of which may be connected to an external circuit (a supply, a load, or a combination of the two). This network has a graph G, with vertices representing nodes of the network and arcs connections. Each arc is assigned an arbitrary direction for the purpose of identifying current and voltage polarities. The analysis technique developed here relies on viewing G as composed of two subgraphs: $G = C \bigcup E$, as indicated in Figure 2–7. Each of the cable segments has associated impedance (resistance) $z_i = r_i$

Loss minimization by discretionary control

In a managed network the current flowing from the power bus into an external circuit is taken to comprise two components:

- the demand component, which is under the control of the external circuit, but subject to authorization from the bus controller; and

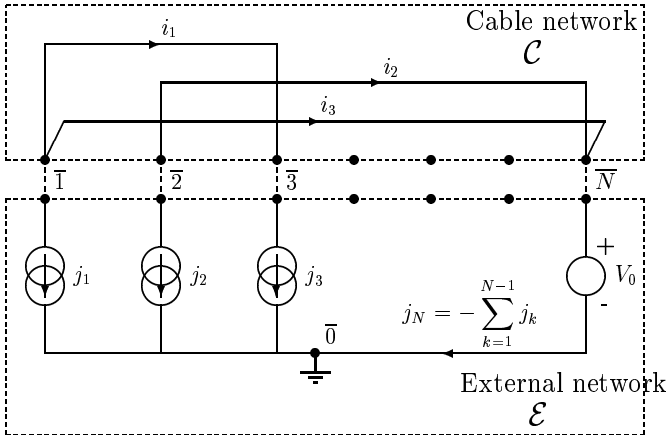

Figure 2–7: A general distribution network.. [46]

- the discretionary component, which is under the control of the bus through current set points transmitted periodically to the external circuit controller.

The discretionary currents as defined in [47]:

"This refers to the ability of a supply or load circuits to control its currents in response to externally determined setpoints. In a conventional distribution system with one point of supply, the supply current is determined for the sum of the various load currents. If there is more than one supply, other factors must be brought to bear on the allocation of current between supplies. Taking this idea to a higher level of abstraction, any load with a controllable setpoint may be thought of as a 'virtual supply', where an increase in the virtual supply current corresponds to a *reduction* in load current brought about by a change in the setpoint."

The demand component of the current is sensed positive flowing from the bus to the external circuit, while the discretionary component is sensed positive flowing from the external circuit to the bus. The sum of all external circuit discretionary ratings is the *capacity* of the system, and sets a limit on the aggregate of all demand requests. Load shedding may potentially occurs when a reduction in its discretionary

rating leads to a reduction in system capacity. The theory developed is applicable to any network in which the external circuits can be modeled as current sinks. The analysis is specialized to managed DC networks by introducing the concept of a *discretionary map*, which expresses the quantitative relationship between discretionary and demand components of current.

The Loss minimization problem is a quadratic (convex) optimization problem with linear constraints, amenable to solution by a number of standard techniques. When applying these techniques, it is convenient to state the problem in the "standard form" [46]. This problem may be solved using the Least Distance Programming (LDP) based on a least-squares approach.

Loss minimization by network reconfiguration

The authors in [45] solved the reconfiguration problem for radial power distribution networks as follows: given a load profile for a distribution network with a number of tie lines and switching points, find a radial configuration for the network which minimizes the network losses . The problem was solved using graph-theoretic framework, where the problem is to find a spanning tree in a graph with weighted nodes and branches, such that an objective function of the weights, obtained by reference to Ohms and Kirchoffs Laws (steady-sate) $\sum z_j i_j^2$, is minimized.

The algorithm takes as input the reduced incidence matrix A of the distribution network with tie lines included, the resistances r_j of each cable segment, and the external circuit current j_k for the first $N-1$ nodes. It begins by determining an initial spanning tree Γ_0 for the given network, and the sensitivity matrix S_0 for the corresponding tree network (obtained by inverting the appropriate submatrix of A). The initial cable currents and losses are also calculated at this point. Starting from these initial conditions, the algorithm generates all the spanning trees for the network. The sensitivity matrix is modified row by row; whenever a row of the matrix

changes, the corresponding cable current is recalculated and the losses perturbed by the difference between the squares of the old and new currents, multiplied by the appropriate cable resistance:

$$P'_{loss} = P_{loss} + r_j(\mid i'_j \mid^2 - \mid i_j \mid^2)$$

In the case of the row corresponding to the arc being substituted, the magnitude of the current is unchanged, and the loss need only be altered to take account of the physical cable substitution:

$$P'_{loss} = P_{loss} + (r_r - r_q) \mid i_m \mid^2$$

After each step the loss is compared with the minimum loss obtained so far, and if not higher, the current configuration is recorded. In those cases where the minimal loss configuration is not unique, the algorithm is capable of reporting all configurations having the same minimal loss.

This algorithm does not take into account operational limits (such as maximum current or power-transfer limits) on individual cable segments, or node voltage constraints.

In general, the literature review on network reconfiguration, does not show reconfiguration of variable loads taking into account the operational limits on electrical power distribution systems (e.g. maximum current or power-transfer limits on each component, or maximum node voltage allowable), and there are no enough works on load shedding algorithms. Then, we work on the reconfiguration of variable loads using graph-theory method, doing a maximization of the power flow in the system under safe operating conditions, and we propose different schemes for load shedding regarding the load priority. Also, the reconfiguration process must be faster; this implies that the number of switching operations is minimized into the algorithm.

2.5 Summary

Different architecture in electrical power distribution systems were presented in this chapter. Zonal distribution architectures provide maximum protection (fault tolerance) than radial distribution, due to the power electronics state of the art, in terms of increase in power density, reliability of power switching, elements with reduced cost, and the invention of advance control technique. On the other hand, this permits fast reconfiguration; for these reasons the EPDS used in this study will be self-contained DC Zonal Electric Distribution Systems.

This chapter also made an introduction of graph theory and its previous applications in reconfiguration of power systems were also introduced. Graph theory can simplify power system representation and represent any system topology changes as a graph operation. Since a DCZEDS is small in area and has possible entire system measurement, graph representation of the system topology is helpful to analyze a system configuration and operation.

CHAPTER 3
Graph Theory and The Reconfiguration Problem

3.1 Overview

The previous chapter presented the state of the art on reconfiguration for power systems, and graph theory was selected to be applied in this research as tool to develop the reconfiguration algorithm. The purpose of this chapter is to define the fundamentals of this theory, and to give a mathematical formulation of the reconfiguration problem planted.

3.2 Problem Formulation

When electric power supply interruption is caused by a fault, it is imperative to reconfigure the power system quickly to a functional configuration after the fault [49]. Reconfiguration functions alter the system topology to meet operational requirements opening and closing switches, load shedding/pickup and adjusting of generators outputs [2]. The reconfiguration problem is defined like an optimization problem where the purpose is to maximize the number of loads served with highest priority, taking into account system constraints to avoid possible overloading of the system and load shedding/pickup.

This thesis is focused in the network behavior in steady state, which means that the specific performance of loads (i.e. dynamic state) is not taking in consideration for a DC Zonal Electric Distribution System. The methodology used during this work is graph-theory, where the reconfiguration problem is solved as a network flow problem where the flow in the network is related to DC electrical signals in steady state.

The next section has some definitions about graph-theory that will be used during the research.

3.3 Graph Theory Concepts

Graph theory is very general and has been used in several applications of power system network representation, simulation, and analysis. This section introduces fundamentals of graph theory:

Definition 1 (Graph)**.** Represented as $G = (N, A)$, where N is a group of *nodes* (or vertex) and A a group of *arcs* (or edges) whose elements are ordered pairs of distinct nodes [54].

The nodes of a graph are usually numbered, says, $1, 2, 3, ..., n$ and typically are designated by circles, with the number inside each circle denoting the index of that node. An arc between nodes i and node j is then represented by pairs (i, j) and are represented by the line between the nodes [41].

Definition 2 (Directed graph)**.** also known as digraph, it has edges that are directed and ordered pairs connecting a source vertex to a target vertex [31]. Figure 3–1 shows an example of a directed graph.

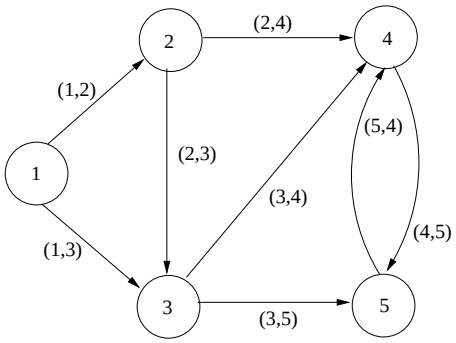

Figure 3–1: Directed Graph

In addition to the visual representation of a directed graph, other common method of representation is in terms of a graph's node-arc incidence matrix.

Definition 3 (Node-Arc Incidence matrix)**.** Represents a graph using a matrix. It is constructed by listing the nodes vertically and the arcs horizontally. Then in the column under arc (i, j), a positive 1, $(+1)$ is placed in the position corresponding to the input node j and a negative 1, (-1) is placed in the position corresponding to the output node i [41]. A Node-Arc Incidence matrix for the graph shown in Figure 3–1 is shown in Table 3–1.

Table 3–1: Node-Arc Incidence matrix representation of Figure 3–1

Node \ Arc	(1,2)	(1,3)	(2,3)	(2,4)	(3,4)	(3,5)	(4,5)	(5,4)
1	-1	-1	0	0	0	0	0	0
2	1	0	-1	-1	0	0	0	0
3	0	1	1	0	-1	-1	0	0
4	0	0	0	1	1	0	-1	1
5	0	0	0	0	0	1	1	-1

There are other important definitions associated with graphs that are useful in describing their structure:

A *chain* between nodes i and j is a sequence of arcs connecting them. The sequence must have the form (i, k_1), (k_1, k_2), (k_2, k_3), $\ldots$,(k_m, j). If a direction of

movement along a chain is specified, say from node i to node j), it is then called a *path* from i to j. A *cycle* is a chain leading from node i back to node i. A graph is a *tree* if it is connected and has no cycles. Sometimes is considering a tree within a graph G, which is just a tree made up a subset of arcs from G. Such a tree is a *spanning tree* if it touches all nodes of G. The notions of paths and cycles can be directly applied to directed graphs. Furthermore, it is possible to say that node j is *reachable* from i if there is a path from node i to j [41].

3.3.1 Network Flow

A *network* is a directed graph that contains weights (numbers) or flows along the arcs [41]. These numbers might represent distance, capacity, voltage, current, resistance, etc., depending on the context. In applications, the network might represent a transportation system or a communication network, or it may simply be a representation used for mathematical purposes.

In an arc (i, j), a *net flow* is a real-valued function $f(i, j)$, that may be thought as an amount of some commodity that can arrive to j from i per unit time, this could be positive or negative. Flows in the arcs of the network must satisfy conservation criterion at each node.

The total flow into a node must be equal to the total flow out of the node, unless the node is a *source*, which has more outgoing flow, or *sink*, which has more incoming flow (or, alternatively, supply nodes or demand nodes).

The value of a flow f out of a source might be positive, and its level might be either fixed or variable [34].

In some network applications, it is useful to assume that there are upper bounds on the allowable flow in various arcs. This introduces the concept of a capacitated

network.

Definition 4 (Capacitated Network)**.** Is a network in which some arcs are assigned nonnegative capacities, which define the maximum allowable flow in those arcs. The capacity of an arc (i, j) is denoted k_{ij}, and this capacity is indicated on the graph by placing the number k_{ij} adjacent to the arc [41].

Definition 5 (Residual Network)**.** Given a flow network, the residual network consists of arcs that can admit more net flow. The amount of available capacity of an arc (i, j) is the *residual capacity* and is given by $kr_{ij} = k_{ij} - f_{ij}$ [18].

The flow and capacity are denoted by f_{ij}/k_{ij}. The network example in Figure 3–1 is now shown in Figure 3–2 with flows and capacities. Notice how the network upholds capacity constraints and flow conservation. The total amount of flow from source (node 1) to sinks (nodes 4 and 5) is 5, which is also the incoming flow to sinks.

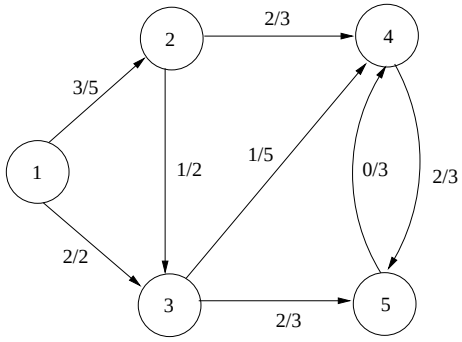

Figure 3–2: Network with flows and capacities f_{ij}/k_{ij}

The residual network for the above network is shown in Figure 3–3.

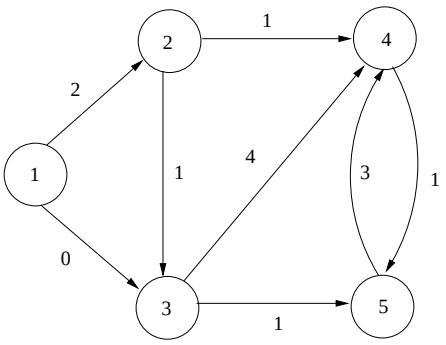

Figure 3–3: Residual Network

3.4 Mathematical Formulation for Reconfiguration of DC Power Distribution Systems

In power systems, different loads provide different services. The loads in the power system have their priorities, based on the importance of the service that a load provides. For example in a ship DC power distribution, the loads used for propulsion generally have higher priority than loads used for laundry services. The priority of load L_i is denoted by variable P_i, which is a number in the range $[1, M]$. This number indicates the relative priority of a given load with respect to other loads in the system [37]; values close to M indicate loads with high priority, whereas values close to 1 indicate loads with low priority.

On other hand, there are two flow definitions to obtain the problem formulation, these are shown in Figure 3–4:

Inflow f_{in}. Represents the power flows into the node i; where (j, i) represents the directed edge from node j to node i.

Outflow f_{out}. Represents the power flows out of the node i; where (i, j) represents the directed edge from node i to node j.

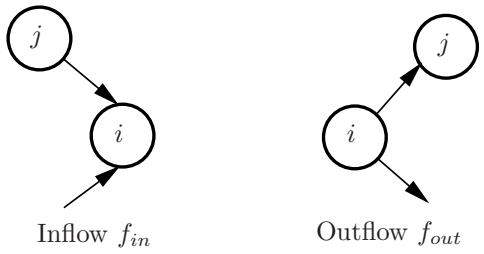

Figure 3–4: Flows on a node i

In this research, the reconfiguration problem is formulated as a multi-objective network flow optimization problem, where two objective functions are considered. The first one is given as a *maximal flow problem*, where the objective is to determine the maximal number of served loads with the highest priority and the second one is to determine the minimum switch operations needed to realize the reconfiguration of the system. The objective functions and constraints for this problem will be discussed in the next section.

3.4.1 Objective Functions

The first objective function is shown in Eq.3.1, which is the sum of the power in the loads l_i (these loads are l_1 to l_n) in the system. The load power flow will be affected by its priority P_i and its status y_i. The contribution of high priority loads is greater than the contribution of a low priority load and the status of the loads should be 1 if the load is energized or 0 if the load is not energized.

$$\textbf{maximize} \quad \sum_{i=1}^{n} y_i P_i l_i \tag{3.1}$$

The second objective function minimizes the number of switching operations n_{ops}, required to move the system topology from the initial post-fault configuration

to the final configuration, a lower value of n_{ops} implies that less time is needed during the network reconfiguration process [30]. This objective function is denoted by Eq.3.2, where N_s represent the total number of switches; S_i and S_{oi} are the number of switches connected at the final and original configuration, respectively.

$$\textbf{minimize} \quad n_{ops}(S_{oi}, S_i) = \sum_{i=1}^{N_s} |S_i - S_{oi}| \tag{3.2}$$

3.4.2 Constraints

In the reconfiguration of the power system, it is necessary to consider physical constraints related to the system operation. These constraints are described in [11] and are as follows:

Source node N_g. May have a net outflow. Also, the sum of the flows going out of the source node should not exceed the total capacity of the respective source node k_i.

$$\sum_{i=1}^{N_g} f_{in} = \sum_{i=1}^{N_g} f_{out} - l_i \tag{3.3}$$

$$\sum_{i=1}^{N_g} f_{out} \leq k_i \tag{3.4}$$

Load node N_l. May have a net inflow.

$$\sum_{i=1}^{N_l} f_{in} = \sum_{i=1}^{N_l} f_{out} + l_i \tag{3.5}$$

Intermediate node N_t. The sum of flows into the node should be equal to sum of the flows coming out of the node.

$$\sum_{i=1}^{N_t} f_{in} = \sum_{i=1}^{N_t} f_{out} \tag{3.6}$$

The outflow of the sources will be equal to the inflow of the loads as a consequence of the conservation at all other nodes.

Variable loads. For any load, the loads could be restored until achieves their maximum value (l_i^{max}).

$$l_i \leq l_i^{max} \tag{3.7}$$

Flow. If the edge is open the flow through it must be zero, otherwise it must not exceed the edge capacity k_{ij}.

$$f_{ij} \leq y_{ij} k_{ij} \tag{3.8}$$

3.5 Proposed Reconfiguration Algorithm

The reconfiguration process is activated by a signal and can run repeatedly at a specified interval of time. The processing diagram of the reconfiguration algorithm is shown in Figure 3–5.

The reconfiguration algorithm contains matrices to represent the graph completely. The algorithm is constantly monitoring fault detection, and when this occurs, the current data of flows and status on each arc are acquired. If the fault is caused by any component failure, this must be isolated. The energized arcs are labeled regarding the connected load priority. The power on each node is evaluated,

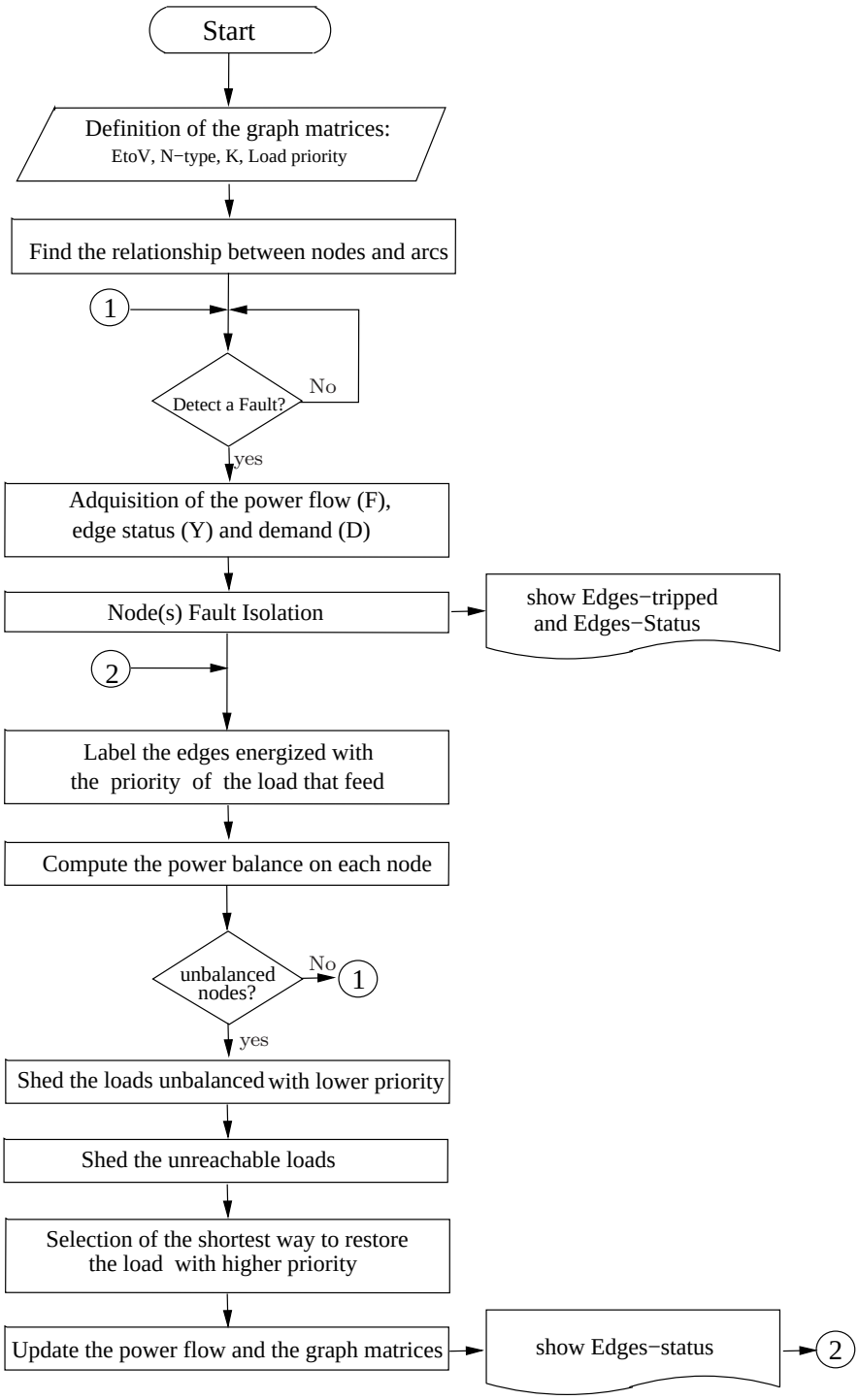

Figure 3–5: Reconfiguration steps

and the reconfiguration process ends if there are not unbalanced nodes, otherwise the process continues. The algorithm has two load shedding schemes; the first one,

sheds loads with lower priority when the generation capacity is not enough to supply all of them; the second one, sheds loads when there are no paths to connect them. The shortest paths are which contain the less quantity of edges to reconfigure the system, and are selected seeking of all the possible paths from generators to loads; grouping the paths according to the load to be connected, and finally these groups are sorted regarding the priority of the loads (first the highest). When a path is selected, the graph matrices are updated and the new system topology is evaluated to verify if the constraints are satisfied. The reconfiguration process ends when there are not unbalanced nodes.

3.6 Summary

This chapter presented the fundamentals of graph theory, which is used during this work, to solve the reconfiguration problem as a network flow problem. The reconfiguration algorithm finds paths that solve the objective functions and satisfies the system constraints defined in the mathematical formulation of the reconfiguration problem. Chapter 4 presents and explain the algorithm itself, and an example using a DC Zonal Electric Distribution System.

CHAPTER 4
Reconfiguration Algorithm for a DCZEDS

4.1 Overview

The previous chapters introduced the background information about DC zonal electric distribution systems DCZEDS, graph theory and its application in power networks. In this chapter we present the reconfiguration algorithm for a DCZEDS.

To begin with the reconfiguration process, it is necessary to define the system elements (generator, load, converters, etc) as elements of the graph (nodes and edges). Next, for complete the graphical representation it is required to enumerate all the nodes and edges of the system. On other hand, the matrices that represent the DCZEDS as a graph model will be defined and others will be introduced to use in the algorithm.
The reconfiguration algorithm will be explained in detail using an application example on a single DCZEDS.

4.2 Reference System

The reference system is the simulation model of an Integrated Power System (IPS), provided by ONR (Office of Naval Research), of the testbed installed at the University of Missouri-Rolla and Purdue University under a related Naval Combat

Survivability initiative [64]. The ship service power is composed of the AC generation and propulsion testbed and DC zonal ship service distribution testbed. The overall ONR reference system configuration is presented in Figure 4–1.

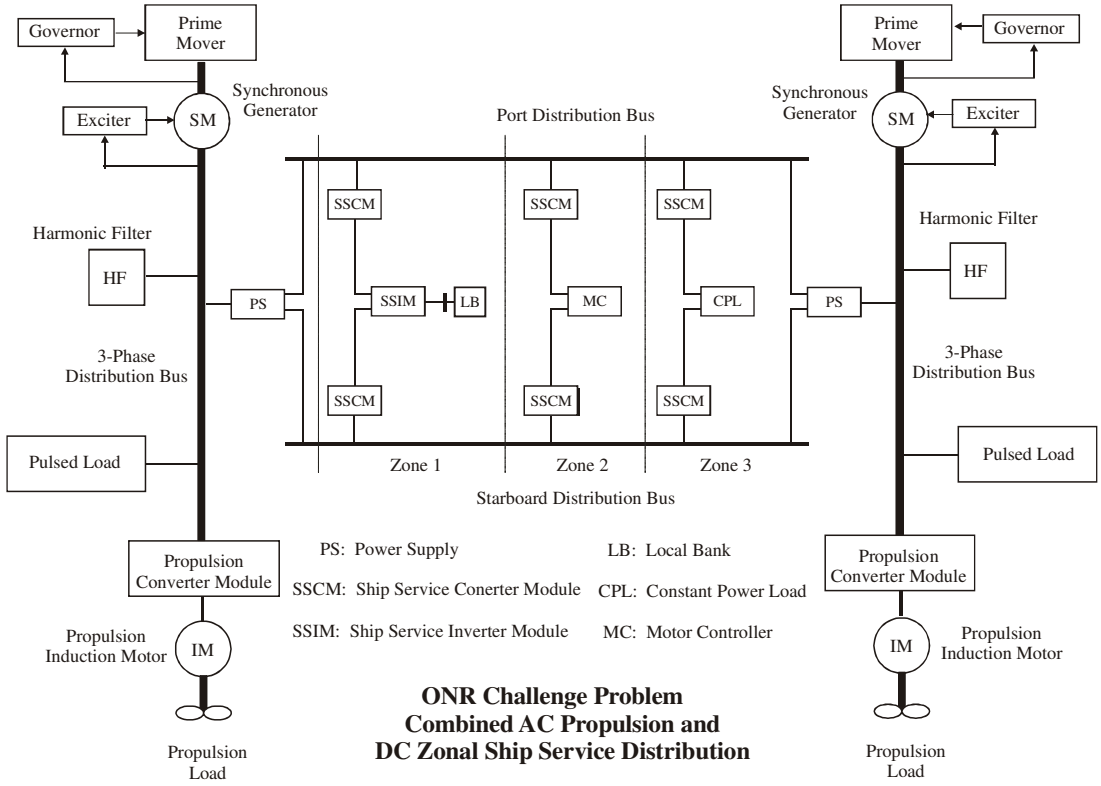

Figure used with permission from Dr. Edwin Zivi

Figure 4–1: ONR Reference System [64]

This research is focused on the DC part of the Integrated Power System, which is shown in Figure 4–2. The DC Zonal Ship Service Distribution Network is based on Dual Bus architecture.

The DC Zonal Ship Service Distribution Network consists of the following elements [64]:

- Each 15 KW ship service power supply (PS) consists of a 480V 3-phase AC diode rectifier bridge feeding a buck converter to produce 500V DC. These converters provide the logical interconnection of the AC and DC testbeds.

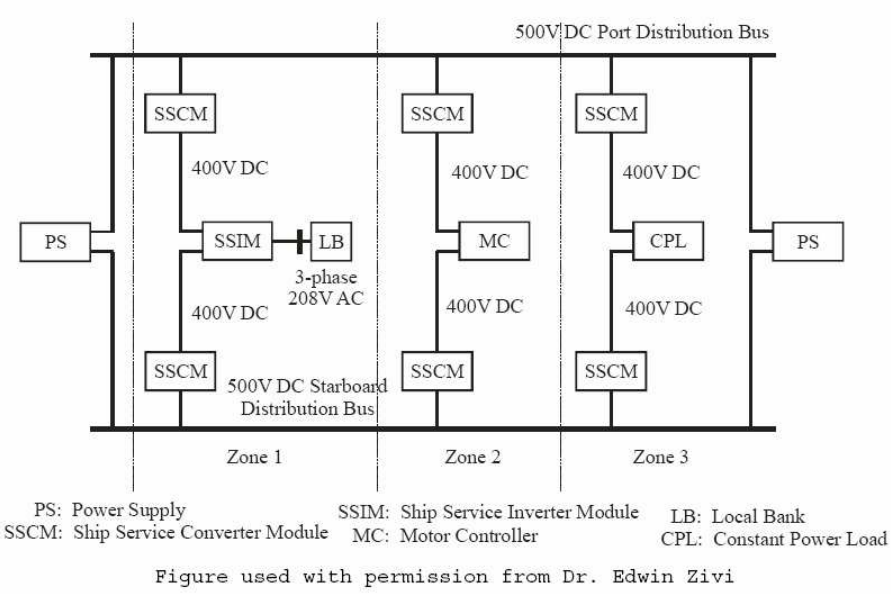

Figure 4–2: DC Zonal Ship Service Distribution Network [64]

- The 5KW ship service converter modules (SSCM)convert 500V DC distribution power to intra-zone distribution of approximately 400V DC.
- The 5KW ship service inverter modules (SSIM) convert the intra-zone 400V DC to three-phase 230V AC power.
- The Motor Controller (MC) is a three-phase inverter rated at 5KW.
- The Constant Power Load (CPL) is a buck converter rated at 5KW.

4.3 Adaptation for a DC Zonal Electric Distribution System

A slight modification to the DCZEDS (ONR-DC Zonal Ship Service Distribution Network) is considered in this study. The adaptation is shown in Figure 4–3 and includes the placement of some switches in order to connect adjacent zones ($S_1 \ldots S_{13}$) and to disconnect loads ($S_{14} \ldots S_{16}$) when load shedding is necessary. They can be opened or closed during reconfiguration when a fault is detected. This would help to isolate a given zone so that the adjacent zones are not affected.

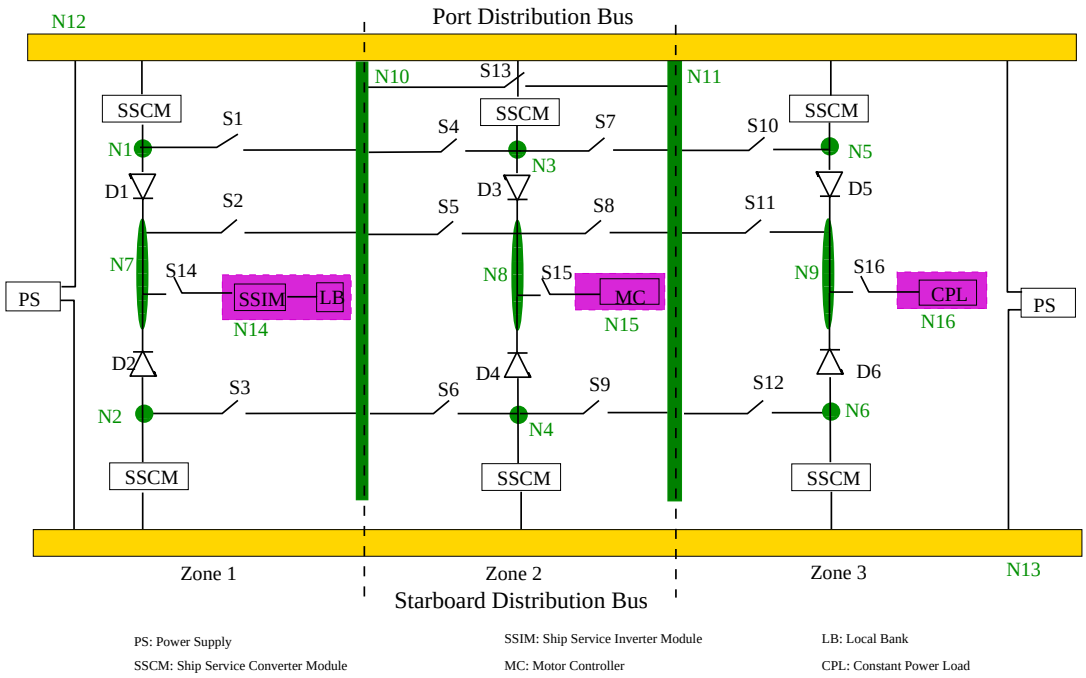

Figure 4–3: Adapted DCZEDS

Also two busses are added to interconnect zones (N_{10} and N_{11}), so we can feed the loads by adjacent zones when is not possible to feed them by their SSCMs. The nodes $N_1 \dots N_9$ indicate electrical nodes of elements interconnection. The port and starboard busses are represented by N_{12} and N_{13} respectively and the load nodes are identified by $N_{14} \dots N_{16}$

The loads are feed by auctioneering diodes ($D_1 \dots D_6$) to ensure that the transfer of power from main bus (port distribution bus) to alternate bus (starboard distribution bus) is seamless and without interruption in case of a fault on one of them [42].

It is important to keep in mind the next considerations for the flow on the switches, SSCMs and Diodes:

- The flow on the switches $S_1 \dots S_{13}$ can travel in both directions.
- The flow on the switches $S_{14} \dots S_{16}$ only goes from the electrical node to the load.
- The flow on SSCM's and Diodes only can goes from the busses to electrical nodes.
- The auctioneering diodes cannot be connected at the same time into the same zone to feed the same load.

4.4 Graph Representation of DCZEDS

As it was mentioned before, this research uses graph theory to simplify power system representation, visualize the system topology and operation, and represent all system topology changes as graph operations.

In order to obtain a graph representation of the power system it is necessary to define the relationship between the major components of the DC Zonal Electric Distribution System showed in Figure 4–3 (generator, load, converters, etc) and the corresponding graph elements (nodes and edges). This relationship is shown in Table 4–1.

Table 4–1: Graph Elements for DCZEDS representation

Components in DCZEDS	Graph Elements
Bus	Node
Generator	Node
Load	Node
Electrical Nodes	Node
SSCM	Edge
Diode	Edge
Switch	Edge

Figure 4–4 shows the modification made to the DCZEDS in Figure 4–3 taking in consideration the Table 4–1, where the components are replaced by nodes (circles) and edges (arrows) enumerated.

As you can see, the bidirectional switches $S_1 \dots S_{13}$ are replaced by two unidirectional edges, this is done to obtain the Node-Edge incidence matrix from the directed graph. The direction of the edges is related to the flux direction of the corresponding connection. Also, the source nodes have been represented as yellow rectangles, the load nodes are purple rectangles, and the intermediate nodes are green circles and rectangles.

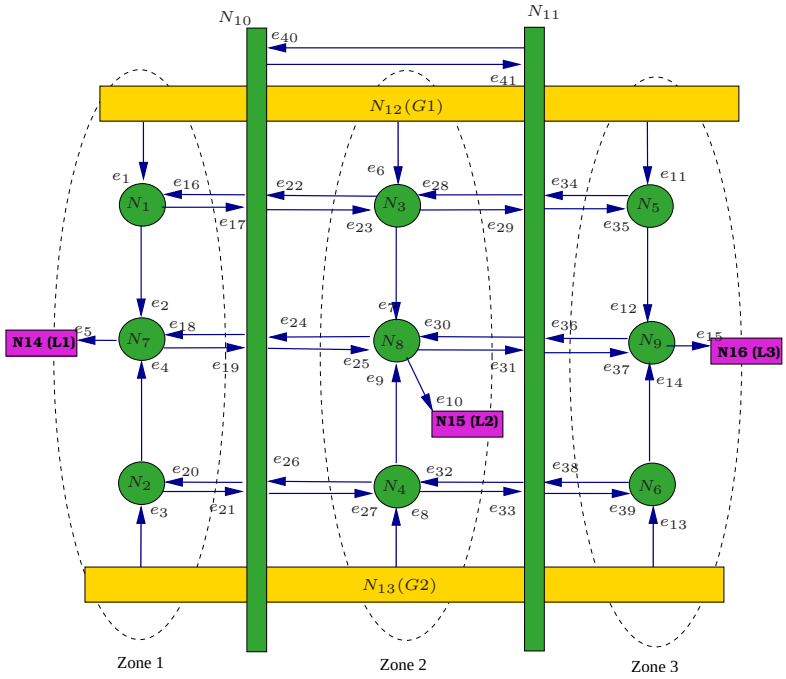

Figure 4–4: Adapted DCZEDS

4.5 Graph Representation for other Power Distribution System

Other kinds of power system network can be represented using graph theory, and any system topology change on the system can be represented as a graph operation.

The graph representations of different power distribution systems are provided in this section to illustrate the generality of this method and the applicability of the algorithm.

4.5.1 Building Integrated Energy System

During the summer of 2007, the Illinois Institute of Technology (ITT) joined forces with several key organizations in the electric power industry and submitted a proposal to the Department of Energy (DOE) to enhance on-site peaking capacity resources in order to improve reliability and security. Distributed resources can reduce peak demand, which can eliminate or defer new transmission and distribution capacity and decrease electricity prices.

The team has focused in the following necessary components of a perfect power system [25]:

- Real-time reconfiguration of power supply assets
- Real-time islanding of critical loads
- Real-time optimization of power supply resources.

The "perfect power" system prototype at IIT includes the following elements:

- Redundant transmission supply
- Redundant area substation supply
- Self-sustaining infrastructure
- intelligent distribution system
- On-site electricity production
- Demand response capability (A/C, lighting, major loads)

- Intelligent perfect power system controller (IPPSC), which will monitor critical parameters to determine the system state and capture trends and will supervise various controls to maintain the system within the specified limits of operation.
- Sustainable energy systems and green buildings/complexes
- Technology-ready infrastructure

The ITT's perfect power prototype builds upon the high reliability distribution system (HRDS) design developed by S&C Electric for the university of California at Santa Barbara is shown in Figure 4–5, which is a loop system that provides high reliability service to each building. In this system any single fault on any of the feeder loops can be isolated without interrupting power. The team separated the campus into logical groups of buildings to maximize reliability and efficiency [25].

In cases where a HRDS system with substation electricity generation cannot be deployed, such as on a radial distribution system, building integrated power systems (BIPS) will provide local generation, power conditioning, and uninterruptible power ride-through capability. The BIPS system, shown in Figure 4–6, will include [25]:

- Local building generation to carry the building load for extended distribution system outage.
- UPS/storage to provide electricity while the local generation is starting.
- Inverters or power quality conditioning devices.
- A load controller to modulate generator output to gradually unload the UPS and to follow the building loads.
- Motor soft-start capability for large motor loads such as elevators.
- Noncritical load-shedding capabilities.
- Communication to the intelligent perfect power system controller (IPPSC).

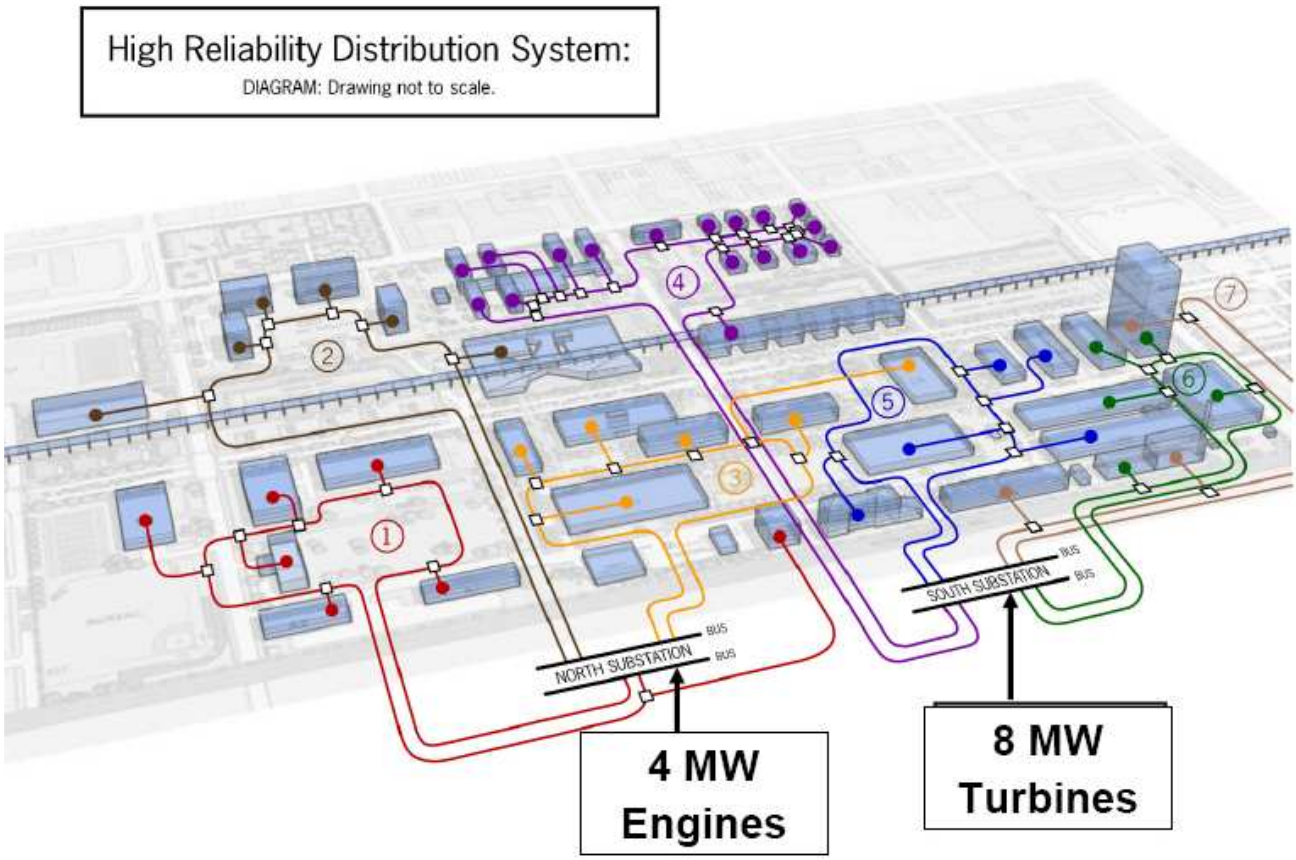

Figure 4–5: High-reliability distribution concept [25]

Figure 4–6 provides a schematic diagram of a typical building energy system for the buildings at IIT. The distribution system consists of two 4,160V feeds from the North Substation. Feeders provide feeder redundancy through switches, which feed into a 500KVA transformer where power is stepped down to 240V. Typically, two panels on each of the three floors distribute electricity to lights, fans and computers [25].

At this point, our interest is to shown the applicability of the graph theory as reconfiguration tool at the building-integrated energy system, this system has a building controller which can be centralized, and each floor can be handled as a

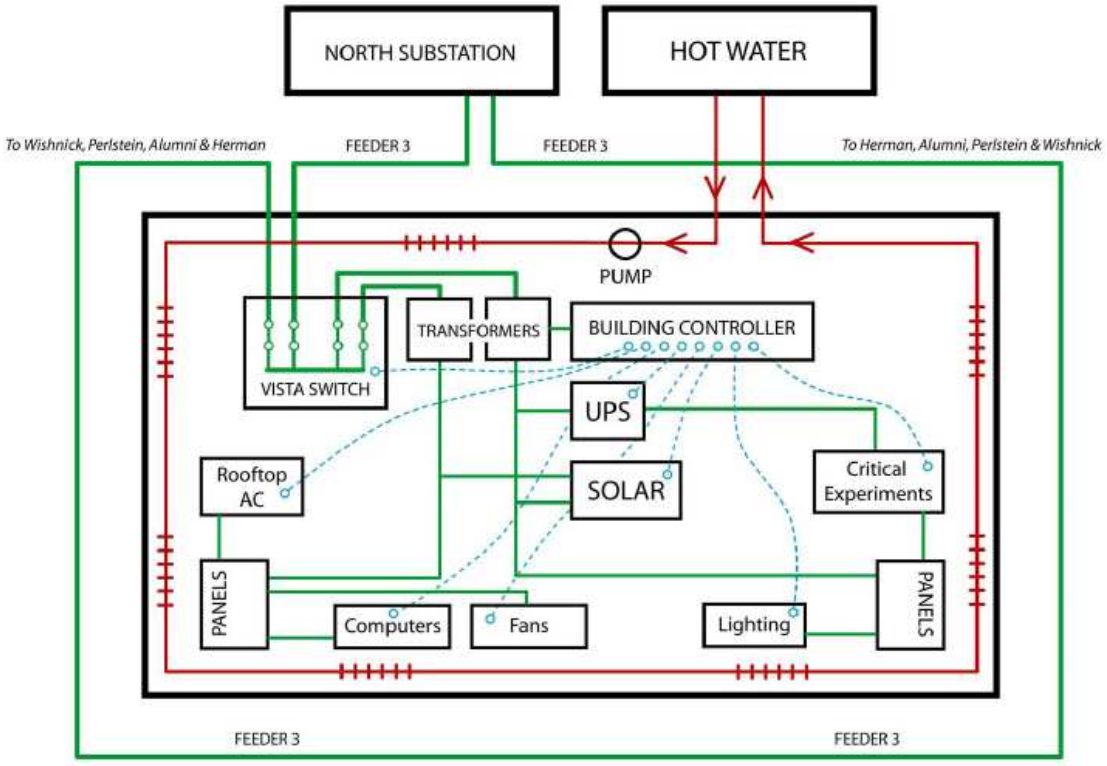

Figure 4–6: Building-integreated energy system [25]

zone. In this case, the BIPS can be represented as a graph doing the relationship between the major components and the corresponding graph elements as is shown in Table 4–2 and the graph representation proposed is shown in Figure 4–7.

Table 4–2: Graph Elements to Represent the BIPS

Components in BIPS	**Graph Elements**
North Substation	Node
Solar PV	Node
Panels	Node
UPS	Node
Electrical Nodes	Node
Lighting	Node
Fans	Node
Computers	Node
Rooftop A/C	Node
Critical experiments	Node
Transformers	Edge
Switch	Edge

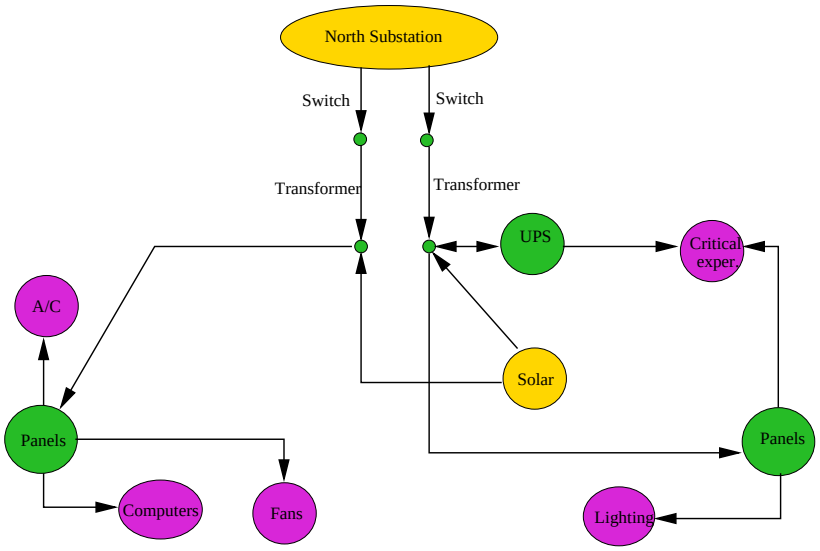

Figure 4–7: Graph representation of the BIPS

4.5.2 Distribution with storage in Zonal Ship

In [20], the author defined a number of key terms, detailed different zonal architectures, described the situations where the architectures are best suited and proposed a framework for zonal ship design to satisfy survivability performance requirements and quality of service requirements.

Our interest is to obtain a graph representation of the Dual bus zonal distribution system (ZDS) with longitudinal bus level storage which is shown in Figure 4–8. This system possesses a dual bus architecture and generation elements in some of the zones. In this system, if one longitudinal bus is damaged, the in-zone conversion/distribution node automatically shifts the source for all the loads to the other longitudinal bus. Typically, at least three generation elements are provided to allow one element to be taken out of service for either damage (survivability) or maintenance (quality of service) while the other two service the tow longitudinal buses. When the generation elements are serving each longitudinal bus and do not have the capacity to service all of the loads, the loads must be shed quickly. If this load shedding is not desired, the total capacity of the generation elements must be

3 times the total load, this can be very expensive. Then, storage elements can be added at the longitudinal buses to supply the loads for the short time needed to restore the system. In this case, each storage element and each generation element must have the capacity of one half of the total load [20].

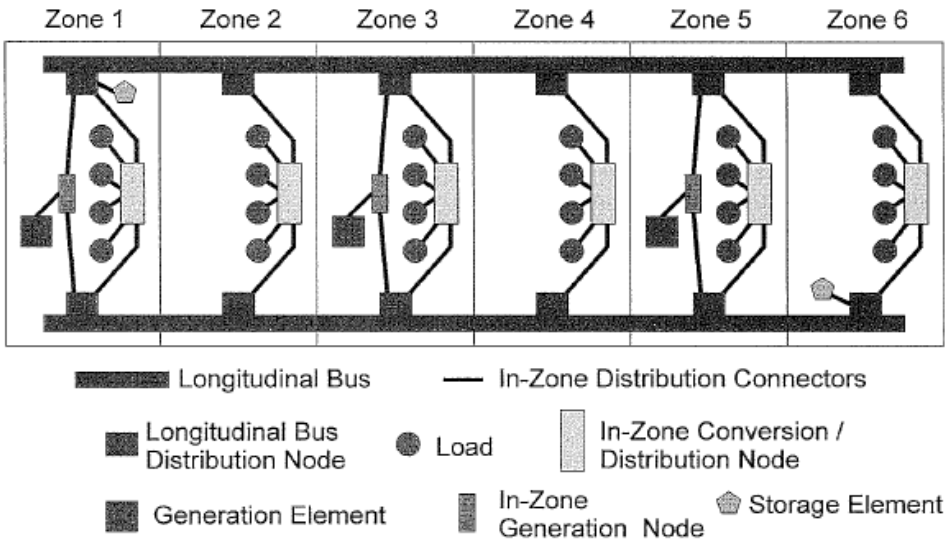

Figure 4–8: Dual Bus Zonal Distribution System with longitudinal bus level storage [20]

The relationship proposed to represent this system in graph is shown in Table 4–3 and its graph representation is shown in Figure 4–9.

Table 4–3: Graph Elements to Represent the Dual Bus ZDS with storage

Components in ZDS with storage	**Graph Elements**
Longitudinal bus (LB)	Node
Longitudinal bus/Distribution node (LD)	Node
Generation element (GE)	Node
In-Zone conversion/Distribution node (CD)	Node
In-Zone generation node (GN)	Node
Storage element (SE)	Node
Load (L)	Node
In-Zone distribution connectors (Cn)	Edge

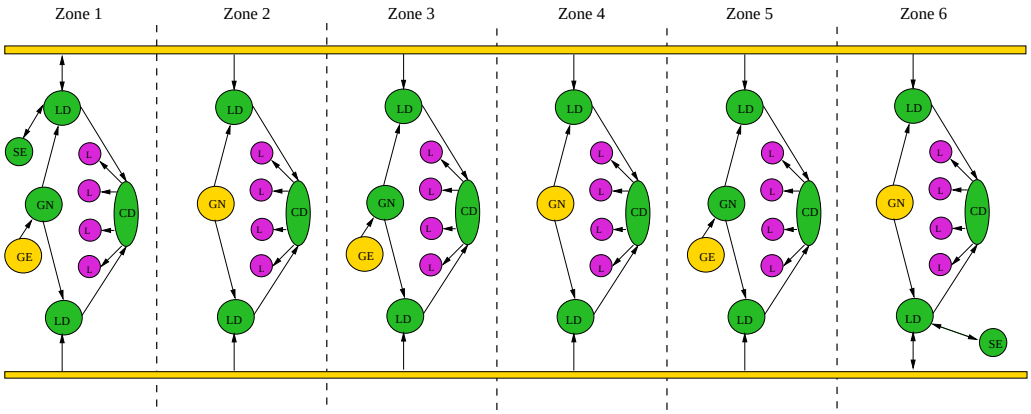

Figure 4–9: Graph representation of the ZDS with storage

4.5.3 Single DCZEDS

Other graph representation is made for a single DCZEDS and it will be used as an application example of the reconfiguration algorithm in this chapter. The graph of the single DCZEDS is a part of the full DCEDS selected in this thesis, and is shown in Figure 4–10, the system only has one generator to supply three SSCMs and three loads. The initial configuration is given when each SSCM feeds its corresponding loads. In this case, the power in steady state flows through the solid lines and the dashed lines are the open switches available to reconfigure the system when a fault occurs. The following assumptions were made:

- Each Ship Service Converter Module (SSCM) has enough capacity to feed one and a half loads ($7.5KW$)
- If one SSCM is damaged, the remaining two SSCM can feed the complete system (three loads).
- The loads are rated at $5KW$ but they can be increased at $15KW$.
- All arcs, except the SSCMs arcs, have the same capacity as the maximum loads power demand ($15KW$).

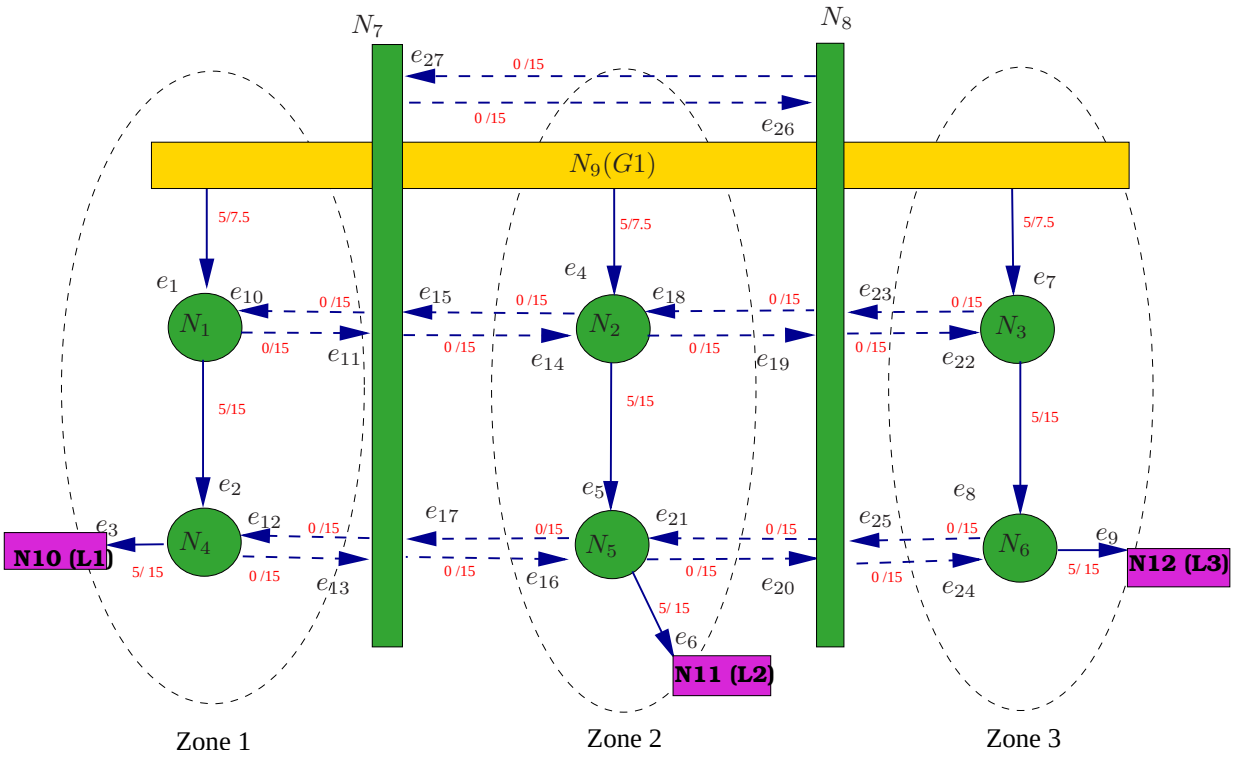

Figure 4–10: Single DCZEDS graph showing initial power flow

4.6 Reconfiguration Algorithm

The reconfiguration algorithm is implemented in Matlab using m-files. The algorithm can be adapted in order to monitor the power system configuration and the power flow through each edge, so the power balance (surplus or deficit) can be calculated in real time when a fault occurs. Under normal conditions, the power flow into a node should equal the power flow out of the node.

4.6.1 Matrices definition

The matrices that represent the DCZEDS as a graph model are defined and introduced into the algorithm. These matrices for the single DCZEDS are:

Node-Edge incidence matrix ($NtoE$) : It is constructed as mentioned in section 3.3 and is shown in Table 4–4. Note that all the edges and nodes (energized

and no energized) are introduced into this matrix.

Table 4–4: Node-Edge Incidence matrix for the single DCZEDS

Node \ Edge	e_1	e_2	e_3	e_4	e_5	e_6	e_7	e_8	e_9	e_{10}	e_{11}	e_{12}	e_{13}	e_{14}	e_{15}	e_{16}	e_{17}	e_{18}	e_{19}	e_{20}	e_{21}	e_{22}	e_{23}	e_{24}	e_{25}	e_{26}	e_{27}
N_1	1	-1	0	0	0	0	0	0	0	1	-1	0	0	0	0	0	0	0	0	0	0	0	0	0	0	0	0
N_2	0	0	0	1	-1	0	0	0	0	0	0	0	0	1	-1	0	0	1	-1	0	0	0	0	0	0	0	0
N_3	0	0	0	0	0	0	1	-1	0	0	0	0	0	0	0	0	0	0	0	0	0	1	-1	0	0	0	0
N_4	0	1	-1	0	0	0	0	0	0	0	0	1	-1	0	0	0	0	0	0	0	0	0	0	0	0	0	0
N_5	0	0	0	0	1	-1	0	0	0	0	0	0	0	0	0	1	-1	0	0	-1	1	0	0	0	0	0	0
N_6	0	0	0	0	0	0	0	1	-1	0	0	0	0	0	0	0	0	0	0	0	0	0	0	1	-1	0	0
N_7	0	0	0	0	0	0	0	0	0	-1	1	-1	1	-1	1	-1	1	0	0	0	0	0	0	0	0	-1	1
N_8	0	0	0	0	0	0	0	0	0	0	0	0	0	0	0	0	0	-1	1	1	-1	-1	1	-1	1	1	-1
N_9	-1	0	0	-1	0	0	-1	0	0	0	0	0	0	0	0	0	0	0	0	0	0	0	0	0	0	0	0
N_{10}	0	0	1	0	0	0	0	0	0	0	0	0	0	0	0	0	0	0	0	0	0	0	0	0	0	0	0
N_{11}	0	0	0	0	0	1	0	0	0	0	0	0	0	0	0	0	0	0	0	0	0	0	0	0	0	0	0
N_{12}	0	0	0	0	0	0	0	0	1	0	0	0	0	0	0	0	0	0	0	0	0	0	0	0	0	0	0

Load priority matrix (L_p): This matrix contains two columns, as is shown in Table 4–5. The first column contains the node numbers that correspond at the loads (N_{10}, N_{11} and N_{12}). The second column contains the priority of each load.

Table 4–5: Load priority matrix for DCZEDS

Node Number	Priority
10	3
11	2
12	1

Node-Type vector(N_t): It is necessary to classify and to select the nodes into the algorithm in order to find the possible paths. This is a column vector matrix (Table 4–6) that contains the node type assigned as follows:

(1) if the node connects a SSCM with a Diode ($N_1 \dots N_3$).

(2) if the node connects a load switch ($N_4 \dots N_6$).

(3) if the node is an interzone node (N_7 and N_8).

(4) if the node is a generator (N_9).

(5) if the node is a load ($N_{10} \dots N_{12}$).

Table 4–6: Node type for single DCZEDS

Node	Type
N_1	1
N_2	1
N_3	1
N_4	2
N_5	2
N_6	2
N_7	3
N_8	3
N_9	4
N_{10}	5
N_{11}	5
N_{12}	5

Capacities vector(k): It is a row vector that contains the maximum flow possible through the edges, see Table 4–7.

Table 4–7: Capacities vector for single DCZEDS

Edge	e_1	e_2	e_3	e_4	e_5	e_6	e_7	e_8	e_9	e_{10}	e_{11}	e_{12}	e_{13}	e_{14}	e_{15}	e_{16}	e_{17}	e_{18}	e_{19}	e_{20}	e_{21}	e_{22}	e_{23}	e_{24}	e_{25}	e_{26}	e_{27}
$k(KW)$	7.5	15	15	7.5	15	15	7.5	15	15	15	15	15	15	15	15	15	15	15	15	15	15	15	15	15	15	15	15

4.6.2 Matrices Acquisition

There are other matrices which can be read by the algorithm when the fault occurs, which are:

Edge-Flux vector (F) : This is a row vector that contains the power flow at the moment that the fault occurs. Table 4–8 shows the power flow for the initial case mentioned in the single DCZEDS presented in Subsection 4.5.3

Table 4–8: Edge-Flux vector for single DCZEDS

Edge	e_1	e_2	e_3	e_4	e_5	e_6	e_7	e_8	e_9	e_{10}	e_{11}	e_{12}	e_{13}	e_{14}	e_{15}	e_{16}	e_{17}	e_{18}	e_{19}	e_{20}	e_{21}	e_{22}	e_{23}	e_{24}	e_{25}	e_{26}	e_{27}
$F(KW)$	5	5	5	5	5	5	5	5	5	0	0	0	0	0	0	0	0	0	0	0	0	0	0	0	0	0	0

Edge-Status vector (Y_s) : It is a row vector that contains a 1 if the edge is connected, or a 0 when the edge is disconnected. The matrix showed in Table 4–9 corresponds at the initial case of the single DCZEDS.

Table 4–9: Edge-Status vector for single DCZEDS

Edge	e_1	e_2	e_3	e_4	e_5	e_6	e_7	e_8	e_9	e_{10}	e_{11}	e_{12}	e_{13}	e_{14}	e_{15}	e_{16}	e_{17}	e_{18}	e_{19}	e_{20}	e_{21}	e_{22}	e_{23}	e_{24}	e_{25}	e_{26}	e_{27}
Y_s	1	1	1	1	1	1	1	1	1	0	0	0	0	0	0	0	0	0	0	0	0	0	0	0	0	0	0

Demand matrix (D)**:** This matrix contains the demand through the edges loads, and is composed by two columns, as shows Table 4–10. The first column contains the edge number that connects each load; the second column contains the corresponding load demand. The load demand corresponds to the power flow through the load just before the fault occurs. If any load has been isolated, the demand of this load keeps the same value before isolation. For this reason, the reconfiguration algorithm is capable of restoring variable loads.

Table 4–10: Demand matrix for single DCZEDS

Edge Number	D (KW)
3	5
6	5
9	5

4.6.3 Steps

The algorithm principal steps or functions are explained as follows:

Nodes-Edges relationship: The first step of the reconfiguration algorithm is to construct the Nodes-Edges relationship matrix; this is an explicit manner to describe the relationship between nodes and edges. This function gives a matrix (VE) with three columns, the two first columns correspond to the nodes (it is not important if are input or output nodes), and the third column shows the edge that connects these two nodes (Table 4–11). The number of rows is equal to the number

of edges in the graph. This matrix is useful to find the reconfiguration paths and to update the flux on each edge.

Table 4–11: Node-Edge relationship Matrix for the single DCZEDS

Node	Node	Edge
1	9	1
1	4	2
1	7	10
1	7	11
2	9	4
2	5	5
2	7	14
2	7	15
2	8	18
2	8	19
3	9	7
3	6	8
3	8	22
3	8	23
4	10	3
4	7	12
4	7	13
5	11	6
5	7	16
5	7	17
5	8	20
5	8	21
6	12	9
6	8	24
6	8	25
7	8	26
7	8	27

Fault detection and isolation: The algorithm detects two kinds of fault:

- Fault by component failure.
- Fault by node overload.

When the algorithm detect fault(s) by overload on any node do not isolate the node with unbalance, then the reconfiguration process continues to the next step. However, when the fault is caused by a component failure, it is necessary to isolate the fault-node(s) (N_2, for the example case); this implies that incidence matrix has smaller dimension. Figure 4–11 shows the graph representation for this case. This function returns the reduced incidence matrix, which is obtained by the elimination of the row(s) corresponding to the fault-node(s) and the columns that correspond

to the edges that connect these nodes (see Table 4–12). The edges surrounding the fault-nodes(s) are detected from the Node-Edges relationship and are placed into a row matrix (Table 4–13). These edges will be disconnected and are not considered for system reconfiguration.

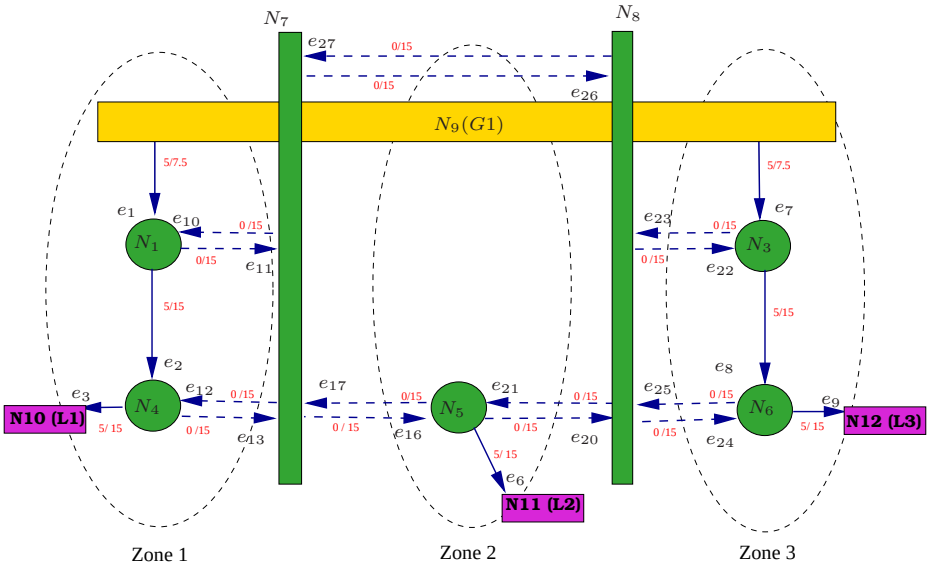

Figure 4–11: Single DCZEDS graph showing fault on N_2

Table 4–12: Node-Edge Incidence matrix updated after isolation of N_2

Node \ Edge	e_1	e_2	e_3	e_6	e_7	e_8	e_9	e_{10}	e_{11}	e_{12}	e_{13}	e_{16}	e_{17}	e_{20}	e_{21}	e_{22}	e_{23}	e_{24}	e_{25}	e_{26}	e_{27}
N_1	1	-1	0	0	0	0	0	1	-1	0	0	0	0	0	0	0	0	0	0	0	0
N_3	0	0	0	0	1	-1	0	0	0	0	0	0	0	0	0	1	-1	0	0	0	0
N_4	0	1	-1	0	0	0	0	0	0	1	-1	0	0	0	0	0	0	0	0	0	0
N_5	0	0	0	-1	0	0	0	0	0	0	0	1	-1	-1	1	0	0	0	0	0	0
N_6	0	0	0	0	0	1	-1	0	0	0	0	0	0	0	0	0	0	1	-1	0	0
N_7	0	0	0	0	0	0	0	-1	1	-1	1	-1	1	0	0	0	0	0	0	-1	1
N_8	0	0	0	0	0	0	0	0	0	0	0	0	0	1	-1	-1	1	-1	1	1	-1
N_9	-1	0	0	0	-1	0	0	0	0	0	0	0	0	0	0	0	0	0	0	0	0
N_{10}	0	0	1	0	0	0	0	0	0	0	0	0	0	0	0	0	0	0	0	0	0
N_{11}	0	0	0	1	0	0	0	0	0	0	0	0	0	0	0	0	0	0	0	0	0
N_{12}	0	0	0	0	0	0	1	0	0	0	0	0	0	0	0	0	0	0	0	0	0

Table 4–13: Edges tripped to isolate N_2

Edges Tripped	[4	5	14	15	18	19]

This step also reduces the node-type matrix, capacities vector, edge-flux vector (Table 4–14) and updates the edge-status vector placing a zero in the tripped

edges (Table 4–15).

Table 4–14: Updated Edge-Flux vector after isolation of N_2

Edge	e_1	e_2	e_3	e_6	e_7	e_8	e_9	e_{10}	e_{11}	e_{12}	e_{13}	e_{16}	e_{17}	e_{20}	e_{21}	e_{22}	e_{23}	e_{24}	e_{25}	e_{26}	e_{27}
$F(KW)$	5	5	5	5	5	5	5	0	0	0	0	0	0	0	0	0	0	0	0	0	0

Table 4–15: Updated Edge-Status vector after isolation of N_2

Edge	e_1	e_2	e_3	e_4	e_5	e_6	e_7	e_8	e_9	e_{10}	e_{11}	e_{12}	e_{13}	e_{14}	e_{15}	e_{16}	e_{17}	e_{18}	e_{19}	e_{20}	e_{21}	e_{22}	e_{23}	e_{24}	e_{25}	e_{26}	e_{27}
Y_s	1	1	1	0	0	1	1	1	1	0	0	0	0	0	0	0	0	0	0	0	0	0	0	0	0	0	0

Label Edges vector: To begin with the reconfiguration procedure, it is important to assign a label for each edge according to the connected load priority (see Table 4–16). If an edge connects various loads, the label assigned corresponds to the highest priority load.

Table 4–16: Updated Edge-Label vector after isolation of N_2

Edge	e_1	e_2	e_3	e_6	e_7	e_8	e_9	e_{10}	e_{11}	e_{12}	e_{13}	e_{16}	e_{17}	e_{20}	e_{21}	e_{22}	e_{23}	e_{24}	e_{25}	e_{26}	e_{27}
Label	0	3	3	2	0	1	1	0	0	0	0	0	0	0	0	0	0	0	0	0	0

Power balance vector: When the fault node(s) is isolated, the power is calculated on each node into the graph. To obtain the power on each node, it is necessary to multiply the flux in the edges by the incidence matrix and then adding the values at each row. The result is a column vector that contains the power on each node.

Table 4–17: Updated Node-Power vector after isolation of N_2

Node	N_1	N_3	N_4	N_5	N_6	N_7	N_8	N_9	N_{10}	N_{11}	N_{12}
Net Power (KW)	0	0	0	-5	0	0	0	-10	5	5	5

This function returns the nodes with negative power balance. These are organized taking into consideration its negative power balance in ascending order (i.e the most negative first). As you can see in Table 4–17, the source node (N_9) and the sink nodes ($N_{10} \dots N_{12}$) have net outflow and net inflow respectively and are not

considered as unbalanced nodes, so the algorithm finds that N_5 has negative power balance.

Find priority: After the unbalanced nodes are founded, the algorithm sorts these nodes considering their priorities and calculates the loads that are possible to feed according to the actual system generating capacity. For the example case, the algorithm finds that all loads can be fed because there is enough capacity in the system.

Shed unbalanced loads: This part of the algorithm disconnects loads using the function `Load-Isolation` explained below. For the example case, the capacity is enough to supply all of the loads and it is not necessary to isolate any of them.

Load Isolation: For the example case, it was not necessary to isolate any load, but sometimes during the reconfiguration process the load shedding must be done under some cases, such as:

- When the generator capacity is not enough to feed all the loads.
- When there are not paths to reach some unbalanced load(s).
- When there are paths that can connect the load but the power flow available is not enough to feed it.

If one or more of these conditions are accomplished the load isolation will be done on the loads with lower priority. This process will reduce the incidence matrix, the edge-flux vector, the node-type matrix and updating the edge-status vector.

Reachability: In cases when there is unbalance in one or more loads, it is not possible to feed some of them due to there are no paths to reach these loads from the SSCMs. Then, it is necessary to detect the reachable loads and continue the reconfiguration process, or detect the loads that are not reachable and disconnect

them. This step of the algorithm uses the function `Find-Paths`, explained below, in order to determine the possible routes or connections that can be done to reconfigure the system. If there are no connections available, the load is isolated and is not considered in the actual reconfiguration process.

Find paths: This is a recursive function that finds all the possible paths from SSCMs to loads and also finds paths from loads to SSCMs. The paths are structures with two fields, which are a cell array of nodes and a cell array of edges. This function returns an array structure that contains all the possible paths.

To find paths from SSCMs to loads, it is necessary to select all the nodes type 1 (see Table 4–6) as initial nodes for each path, then all the connections that enable the power flow to the loads are found taking in consideration the edges that go out from the nodes until arriving to any load node. When the function obtains a set of nodes and edges that connect a load, they are stored as a valid path.

Path Selection: When all the possible paths to feed all the loads are found, it is necessary to select the path that minimize the switching operations and feed the loads with highest priority. This selection is made by ordering the paths taking in consideration the load priority and at the same time the shortest route. The paths given by the reconfiguration algorithm to feed N_5 are shown in Table 4–18. The column indicates all the possible routes from each converter to achieve the loads.

Table 4–18: Paths available to feed N_5

From $\boldsymbol{N_1}$		From $\boldsymbol{N_3}$	
Edges	Nodes	Edges	Nodes
[16 11]	[5 7 1]	[21 23]	[5 8 3]
[16 13 2]	[5 7 4 1]	[16 27 23]	[5 7 8 3]
[21 26 11]	[5 8 7 1]	[21 25 8]	[5 8 6 3]
[21 26 13 2]	[5 8 7 4 1]	[16 27 25 8]	[5 7 8 6 3]

The first step is to select the paths that connect the loads with higher priority and if there are various paths that can feed the load, the one that contains less quantity of edges will be selected. Once the paths are selected, these are evaluated in order to verify that the system constraints are satisfied. When the selected path does not ensure these constraints another path is selected. This evaluation is made by updating the flux each time that any path is connected, and is explained in the function `Update-Flux`.

The paths selected to feed the N_5 are shown in Table 4–19, in this case it was necessary to select two paths in order to supply all the load power demand.

Table 4–19: Paths selected to balance N_5

From $\boldsymbol{N_1}$		From $\boldsymbol{N_3}$	
Edges	Nodes	Edges	Nodes
[16 11]	[5 7 1]	[21 23]	[5 8 3]

Update-Flux: When a path is selected, a new distribution of power flow is made on the graph. This distribution is made by taking into account the edge labels with higher priority and the residual graph, see Section 3.3.1.

On other way, the incidence matrix is increased adding the rows and columns that correspond at the nodes and edges of the path respectively, and the flux, status, capacity and demand matrices are also updated. As a result, the available generator capacity decreases because the power flow increases. The next path to be selected will have these changes in consideration.

The Figure 4–12 shows the paths to balance the N_5 (red solid lines), and the power flow and the capacities updated.

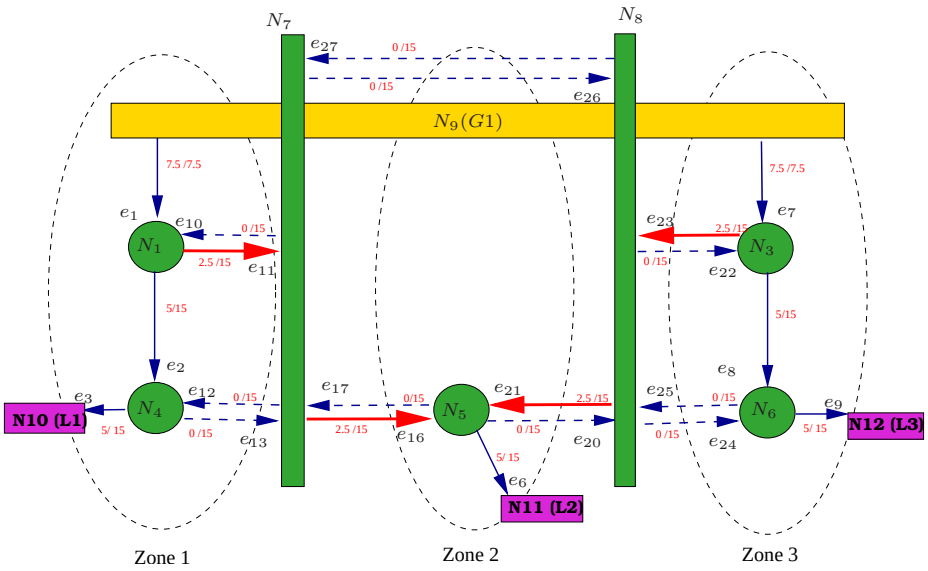

Figure 4–12: Reconfiguration of the single DCZEDS graph with fault on N_2

The status, flux, and power balance matrices are updated and shown in Tables 4–20, 4–21, and 4–22 respectively. Note that the N_5 is balanced and the net power on each node satisfies the system constraints, also the power flow going out of the generator N_{12} is equal to the sum of power flow coming to the load nodes N_{13}, N_{14} and N_{15} . At this point the reconfiguration process ends and the algorithm keeps running until this finds another fault and starts with the reconfiguration process again.

Table 4–20: Updated Edge-Status Vector after restoration of N_5

Edge	e_1	e_2	e_3	e_4	e_5	e_6	e_7	e_8	e_9	e_{10}	e_{11}	e_{12}	e_{13}	e_{14}	e_{15}	e_{16}	e_{17}	e_{18}	e_{19}	e_{20}	e_{21}	e_{22}	e_{23}	e_{24}	e_{25}	e_{26}	e_{27}
Y_s	1	1	1	0	0	1	1	1	1	0	1	0	0	0	0	1	0	0	0	0	1	0	1	0	0	0	0

Table 4–21: Updated Edge-Flux Vector after restoration of N_5

Edge	e_1	e_2	e_3	e_6	e_7	e_8	e_9	e_{10}	e_{11}	e_{12}	e_{13}	e_{16}	e_{17}	e_{20}	e_{21}	e_{22}	e_{23}	e_{24}	e_{25}	e_{26}	e_{27}
$F(KW)$	7.5	5	5	5	7.5	5	5	0	2.5	0	0	2.5	0	0	2.5	0	2.5	0	0	0	0

Table 4–22: Updated Node-Power Vector after restoration of N_5

Node	N_1	N_3	N_4	N_5	N_6	N_7	N_8	N_9	N_{10}	N_{11}	N_{12}
Net Power (KW)	0	0	0	0	0	0	0	-15	5	5	5

4.7 Summary

This chapter discussed the reconfiguration algorithm used to serve as many loads as possible under the maximization problem of a DCZEDS. The reconfiguration process started defining the system elements (generator, load, converters, etc) as elements of the graph (nodes and edges). The matrices that represent the DCZEDS as a graph model were defined and introduced into the algorithm.

This algorithm was capable to isolate the fault node and displayed the edges to be tripped, to evaluate the power balance on each node as result of the fault(s), and to obtain the post-fault reconfiguration system considering the capacitated and residual networks. This reconfiguration algorithm has the capability to shed loads under three schemes if it is necessary. Once a new reconfiguration path was found the new topology was evaluated again to verify if the system constraints were satisfied.

CHAPTER 5
Test Cases and Results

5.1 Overview

This chapter presents the reconfiguration algorithm tested on the DCZEDS for different fault scenarios considering load shedding based on load priorities and unreachability. Also, the reconfiguration when there are increments or decrements on loads power demand will be analyzed in the chapter.

5.2 Load shedding by lower priority in the single DCZEDS

This scenario is running on the single DCZEDS considering the results in the example presented in the previous chapter. Now, a fault occurs on SSCM 3 (represented on N_3) after the load 2 has been balanced after the fault occurred on N_2. Figure 5–1 shows the graph representation for this scenario.

The final matrices show in Section 4.6.3 will be the initial matrices to begin the reconfiguration process when the fault N_3 occurs. These matrices are take up again in Tables 5–1, 5–2 and 5–3

Table 5–1: Edge-Status vector of single DCZEDS at the moment of fault on N_3.

Edge	e_1	e_2	e_3	e_4	e_5	e_6	e_7	e_8	e_9	e_{10}	e_{11}	e_{12}	e_{13}	e_{14}	e_{15}	e_{16}	e_{17}	e_{18}	e_{19}	e_{20}	e_{21}	e_{22}	e_{23}	e_{24}	e_{25}	e_{26}	e_{27}
Y_s	1	1	1	0	0	1	1	1	1	0	1	0	0	0	0	1	0	0	0	0	1	0	1	0	0	0	0

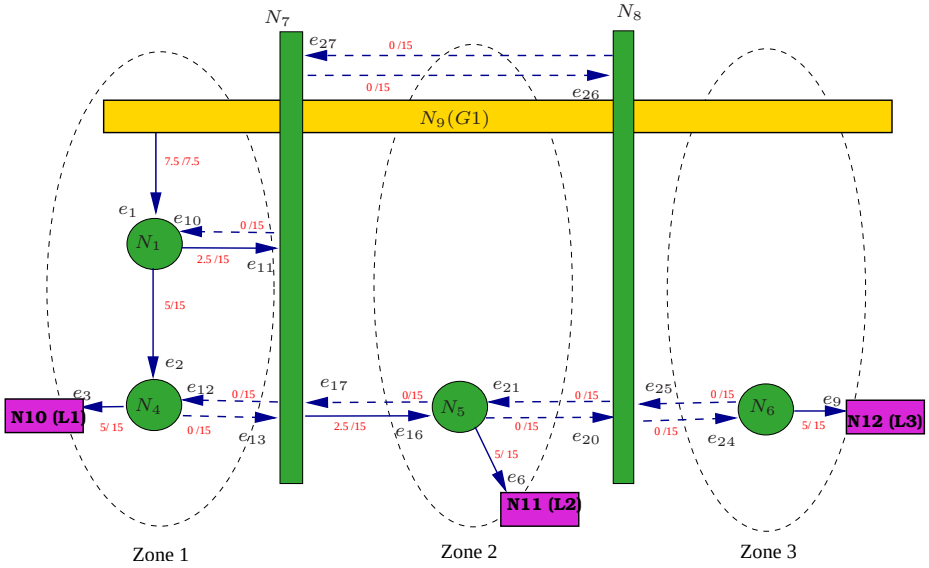

Figure 5–1: Single DCZEDS graph with fault on N_3.

Table 5–2: Edge-Flux vector of single DCZEDS at the moment of fault on N_3.

Edge	e_1	e_2	e_3	e_6	e_7	e_8	e_9	e_{10}	e_{11}	e_{12}	e_{13}	e_{16}	e_{17}	e_{20}	e_{21}	e_{22}	e_{23}	e_{24}	e_{25}	e_{26}	e_{27}
F(KW)	7.5	5	5	5	7.5	5	5	0	2.5	0	0	2.5	0	0	2.5	0	2.5	0	0	0	0

Table 5–3: Demand matrix of single DCZEDS at the moment of fault on N_3.

Edge Number	D (KW)
3	5
6	5
9	5

To isolate the node fault N_3 it was necessary to trip the edges shown in Table 5–4.

After the isolation of node N_3, the edge-flux and edge-status were updated as shown in Table 5–5 and 5–6 respectively, and as a result of the fault, the system presents unbalance on nodes N_5 and N_6 as shown in Table 5–7.

Table 5–4: Edges tripped to isolate N_3.

Edges Tripped	[7 8 22 23]

In this case, the algorithm detects that the SSCM 1 (N_2) is the only one that can handle the generating capacity, this means that the capacity available to supply

Table 5–5: Edge-Flux vector updated after isolation of the N_3.

Edge	e_1	e_2	e_3	e_6	e_9	e_{10}	e_{11}	e_{12}	e_{13}	e_{16}	e_{17}	e_{20}	e_{21}	e_{24}	e_{25}	e_{26}	e_{27}
$F(KW)$	7.5	5	5	5	5	0	2.5	0	0	2.5	0	0	0	0	0	0	0

Table 5–6: Edge-Status vector updated after isolation of N_3.

Edge	e_1	e_2	e_3	e_4	e_5	e_6	e_7	e_8	e_9	e_{10}	e_{11}	e_{12}	e_{13}	e_{14}	e_{15}	e_{16}	e_{17}	e_{18}	e_{19}	e_{20}	e_{21}	e_{22}	e_{23}	e_{24}	e_{25}	e_{26}	e_{27}
Y_s	1	1	1	0	0	1	0	0	1	0	1	0	0	0	0	1	0	0	0	0	0	0	0	0	0	0	0

Table 5–7: Node-Power vector updated after isolation of N_3.

Node	N_1	N_4	N_5	N_6	N_7	N_8	N_9	N_{10}	N_{11}	N_{12}
Net Power (KW)	0	0	-2,5	-5	0	0	-7.5	5	5	5

the remainder system is of $K_t = 7.5KW$. Then, there is not enough power to feed all of the loads power demand ($D_t = 15KW$). Considering the priority of the system loads (balanced or unbalanced, connected or disconnected), it is possible to feed only the load 1 (N_{10}); loads 2 and 3 (N_{11} and N_{12}) must be shed because of their priority level.

To shed these loads, the algorithm must find the paths that feed them from SSCM and disconnect the edges in these paths. Table 5–8 shows the disconnected edges and the current status of the edges is shown in Table 5–9.

Table 5–8: Edges disconnected to shed N_{11} and N_{12}.

Edges disconnected	[6 9 11 16]

Table 5–9: Edge-Status vector updated after load shedding.

Edge	e_1	e_2	e_3	e_4	e_5	e_6	e_7	e_8	e_9	e_{10}	e_{11}	e_{12}	e_{13}	e_{14}	e_{15}	e_{16}	e_{17}	e_{18}	e_{19}	e_{20}	e_{21}	e_{22}	e_{23}	e_{24}	e_{25}	e_{26}	e_{27}
Y_s	1	1	1	0	0	0	0	0	0	0	0	0	0	0	0	0	0	0	0	0	0	0	0	0	0	0	0

Therefore, the power flow after load shedding is updated and is shown in Table 5–10. The new power balance shown in Table 5–11 is calculated to verify the system constrains.

Table 5–10: Edge-Flux vector updated after load shedding.

Edge	e_1	e_2	e_3	e_6	e_9	e_{10}	e_{11}	e_{12}	e_{13}	e_{16}	e_{17}	e_{20}	e_{21}	e_{24}	e_{25}	e_{26}	e_{27}
$F(KW)$	5	5	5	0	0	0	0	0	0	0	0	0	0	0	0	0	0

Table 5–11: Node-Power Matrix updated after load shedding.

Node	N_1	N_3	N_4	N_5	N_6	N_7	N_8	N_9	N_{10}	N_{11}	N_{12}
Net Power (KW)	0	0	0	0	0	0	0	-5	5	0	0

At this point, the algorithm found that power is balanced in all nodes and the reconfiguration process is ended. Figure 5–2 shows the final graph with loads shed when faults occur on N_2 and N_3 with power flow and capacities updated.

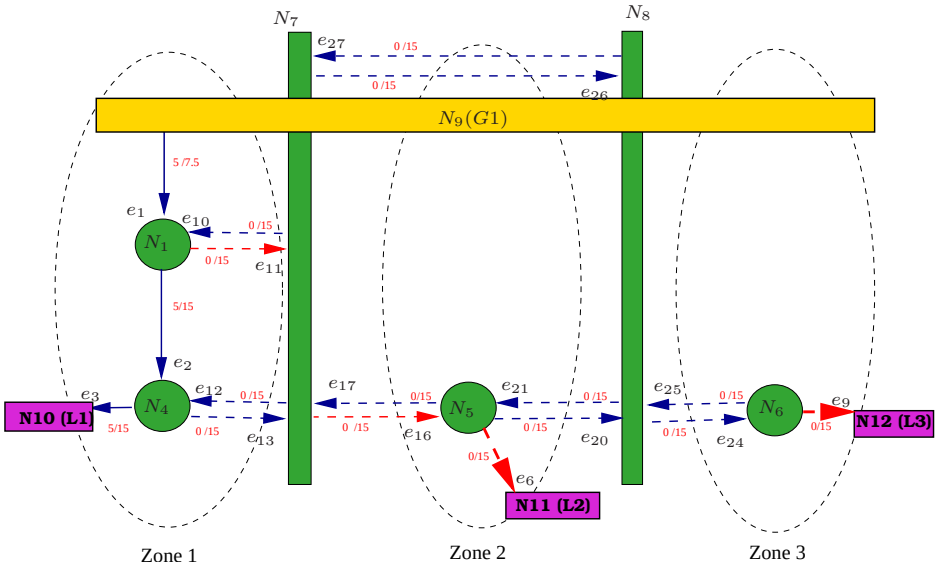

Figure 5–2: Reconfiguration of the single DCZEDS graph with faults on N_2 and N_3.

5.3 Scenarios in full DCZEDS

Three additional scenarios are created for the full DC zonal electric distribution system shown in Figure 4-4 which has the incidence matrix shown in Table 5–12.

In Table 5–13, the node-type vector for this system is shown, taking in consideration:

(1) if the node connects SSCM with Diode ($N_1 \dots N_6$).

(2) if the node connects the load switch ($N_7 \dots N_9$).

Table 5–12: Node-Edge Incidence matrix for the full DCZEDS.

Node \ Edge	e_1	e_2	e_3	e_4	e_5	e_6	e_7	e_8	e_9	e_{10}	e_{11}	e_{12}	e_{13}	e_{14}	e_{15}	e_{16}	e_{17}	e_{18}	e_{19}	e_{20}	e_{21}	e_{22}	e_{23}	e_{24}	e_{25}	e_{26}	e_{27}	e_{28}	e_{29}	e_{30}	e_{31}	e_{32}	e_{33}	e_{34}	e_{35}	e_{36}	e_{37}	e_{38}	e_{39}	e_{40}	e_{41}
N_1	1	-1	0	0	0	0	0	0	0	0	0	0	0	0	0	1	-1	0	0	0	0	0	0	0	0	0	0	0	0	0	0	0	0	0	0	0	0	0	0
N_2	0	0	1	-1	0	0	0	0	0	0	0	0	0	0	0	0	0	0	0	1	-1	0	0	0	0	0	0	0	0	0	0	0	0	0	0	0	0	0	0
N_3	0	0	0	0	0	1	-1	0	0	0	0	0	0	0	0	0	0	0	0	0	0	-1	1	0	0	0	0	1	-1	0	0	0	0	0	0	0	0	0	0
N_4	0	0	0	0	0	0	0	1	-1	0	0	0	0	0	0	0	0	0	0	0	0	0	0	0	-1	1	0	0	0	0	1	-1	0	0	0	0	0	0	0
N_5	0	0	0	0	0	0	0	0	0	0	1	-1	0	0	0	0	0	0	0	0	0	0	0	0	0	0	0	0	0	0	0	0	-1	1	0	0	0	0	0
N_6	0	0	0	0	0	0	0	0	0	0	0	0	1	-1	0	0	0	0	0	0	0	0	0	0	0	0	0	0	0	0	0	0	0	0	0	0	-1	1	0	0
N_7	0	1	0	1	-1	0	0	0	0	0	0	0	0	0	0	0	0	1	-1	0	0	0	0	0	0	0	0	0	0	0	0	0	0	0	0	0	0	0	0
N_8	0	0	0	0	0	0	1	0	1	-1	0	0	0	0	0	0	0	0	0	0	0	0	-1	1	0	0	0	0	1	-1	0	0	0	0	0	0	0	0	0
N_9	0	0	0	0	0	0	0	0	0	0	0	1	0	1	-1	0	0	0	0	0	0	0	0	0	0	0	0	0	0	0	0	0	0	0	0	-1	1	0	0	0
N_{10}	0	0	0	0	0	0	0	0	0	0	0	0	0	0	0	-1	1	-1	1	-1	1	1	-1	1	-1	1	-1	0	0	0	0	0	0	0	0	0	0	1	-1
N_{11}	0	0	0	0	0	0	0	0	0	0	0	0	0	0	0	0	0	0	0	0	0	0	0	0	0	0	-1	1	-1	1	-1	1	1	-1	1	-1	1	-1	-1	1
N_{12}	-1	0	0	0	0	-1	0	0	0	0	-1	0	0	0	0	0	0	0	0	0	0	0	0	0	0	0	0	0	0	0	0	0	0	0	0	0	0	0	0	0
N_{13}	0	0	-1	0	0	0	0	-1	0	0	0	0	-1	0	0	0	0	0	0	0	0	0	0	0	0	0	0	0	0	0	0	0	0	0	0	0	0	0	0	0
N_{14}	0	0	0	0	1	0	0	0	0	0	0	0	0	0	0	0	0	0	0	0	0	0	0	0	0	0	0	0	0	0	0	0	0	0	0	0	0	0	0	0
N_{15}	0	0	0	0	0	0	0	0	0	1	0	0	0	0	0	0	0	0	0	0	0	0	0	0	0	0	0	0	0	0	0	0	0	0	0	0	0	0	0	0
N_{16}	0	0	0	0	0	0	0	0	0	0	0	0	0	0	1	0	0	0	0	0	0	0	0	0	0	0	0	0	0	0	0	0	0	0	0	0	0	0	0	0

Table 5–13: Node type N_t for the full DCZEDS.

Node	Type
N_1	1
N_2	1
N_3	1
N_4	1
N_5	1
N_6	1
N_7	2
N_8	2
N_9	2
N_{10}	3
N_{11}	3
N_{12}	4
N_{13}	4
N_{14}	5
N_{15}	5
N_{16}	5

(3) if the node is an interzone node (N_{10} and N_{11}).

(4) if the node is a generator (N_{12} and N_{13}).

(5) if the node is a load ($N_{14} \dots N_{16}$).

The next restrictions need to be meeting during reconfiguration of the system when a fault occurs:

- Each Ship Service Converter Module (SSCM) has enough capacity to feed one and a half loads ($7.5KW$)
- If one SSCM is damaged, two SSCM's can feed the complete system (three loads).
- The loads are rated at $5KW$ but they can be increased at $15KW$.
- All arcs, except the SSCMs arcs, have the same capacity as the maximum loads power demand ($15KW$).

- The priority of the three loads, are the same as in the single DCZEDS discussed in Table 4–5.

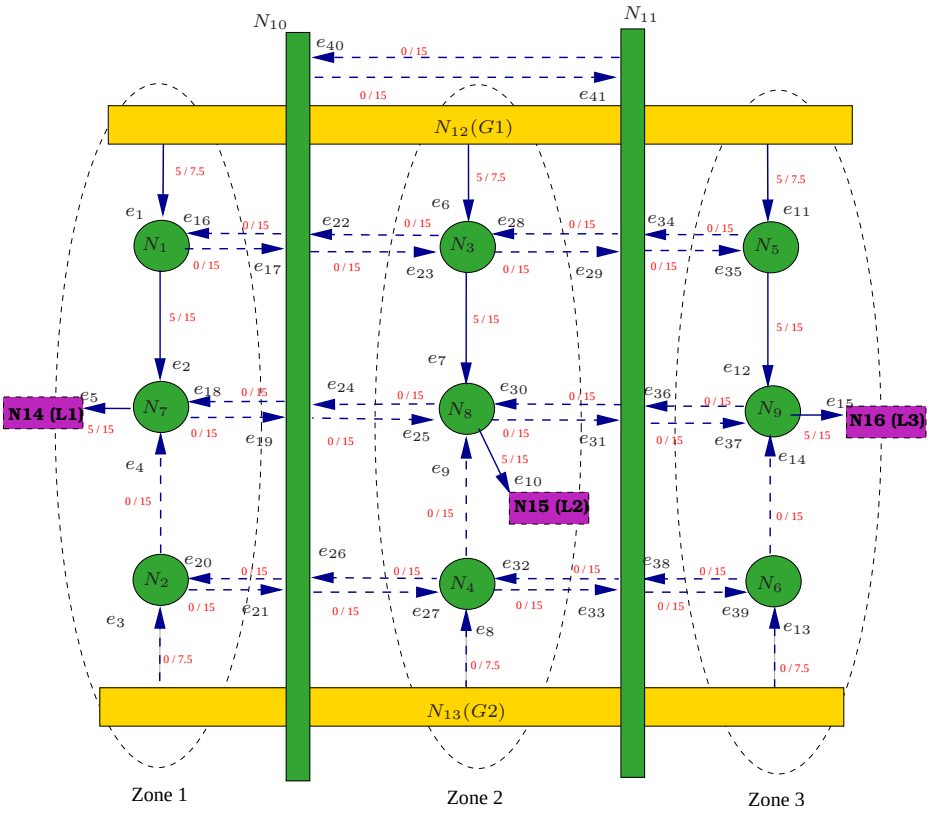

Figure 5–3: Full DCZEDS initial configuration.

The initial configuration of the full DCZEDS is when all SSCM's connected at the main bus N_{12} (port distribution bus) feed their corresponding load, see Figure 5–3. The vectors edge-flux, status, and capacities are shown in Tables 5–14, 5–15 and 5–16 respectively.

5.3.1 Zone Isolation

The first scenario is when three faults occur simultaneously in nodes N_1, N_2 and N_{10}. The isolation of the three faulty nodes is shown in Figure 5–4 and the edges tripped by the algorithm are shown in Table 5–17.

Table 5–14: Initial Edge-Flux vector for the full DCZEDS.

Edge	e_1	e_2	e_3	e_4	e_5	e_6	e_7	e_8	e_9	e_{10}	e_{11}	e_{12}	e_{13}	e_{14}	e_{15}	e_{16}	e_{17}	e_{18}	e_{19}	e_{20}	e_{21}	e_{22}	e_{23}	e_{24}	e_{25}	e_{26}	e_{27}	e_{28}	e_{29}	e_{30}	e_{31}	e_{32}	e_{33}	e_{34}	e_{35}	e_{36}	e_{37}	e_{38}	e_{39}	e_{40}	e_{41}
$\boldsymbol{F(KW)}$	5	5	0	0	5	5	5	0	0	5	5	5	0	0	5	0	0	0	0	0	0	0	0	0	0	0	0	0	0	0	0	0	0	0	0	0	0	0	0

Table 5–15: Initial Edge-Status vector for the full DCZEDS.

Edge	e_1	e_2	e_3	e_4	e_5	e_6	e_7	e_8	e_9	e_{10}	e_{11}	e_{12}	e_{13}	e_{14}	e_{15}	e_{16}	e_{17}	e_{18}	e_{19}	e_{20}	e_{21}	e_{22}	e_{23}	e_{24}	e_{25}	e_{26}	e_{27}	e_{28}	e_{29}	e_{30}	e_{31}	e_{32}	e_{33}	e_{34}	e_{35}	e_{36}	e_{37}	e_{38}	e_{39}	e_{40}	e_{41}
$\boldsymbol{Y_s}$	1	1	0	0	1	1	1	0	0	1	1	1	0	0	1	0	0	0	0	0	0	0	0	0	0	0	0	0	0	0	0	0	0	0	0	0	0	0	0

Table 5–16: Initial Capacities vector for the full DCZEDS.

Edge	e_1	e_2	e_3	e_4	e_5	e_6	e_7	e_8	e_9	e_{10}	e_{11}	e_{12}	e_{13}	e_{14}	e_{15}	e_{16}	e_{17}	e_{18}	e_{19}	e_{20}	e_{21}	e_{22}	e_{23}	e_{24}	e_{25}	e_{26}	e_{27}	e_{28}	e_{29}	e_{30}	e_{31}	e_{32}	e_{33}	e_{34}	e_{35}	e_{36}	e_{37}	e_{38}	e_{39}	e_{40}	e_{41}
$\boldsymbol{k}(KW)$	7.5	15	15	15	15	7.5	15	15	15	15	7.5	15	15	15	15	15	15	15	15	15	15	15	15	15	15	15	15	15	15	15	15	15	15	15	15	15	15	15	15

Table 5–17: Edge tripped to isolate N_1, N_2 and N_{10}.

Edges Tripped	[1	2	3	4	16	17	18	19	20	21	22	23	24	25	26	27	40	41]

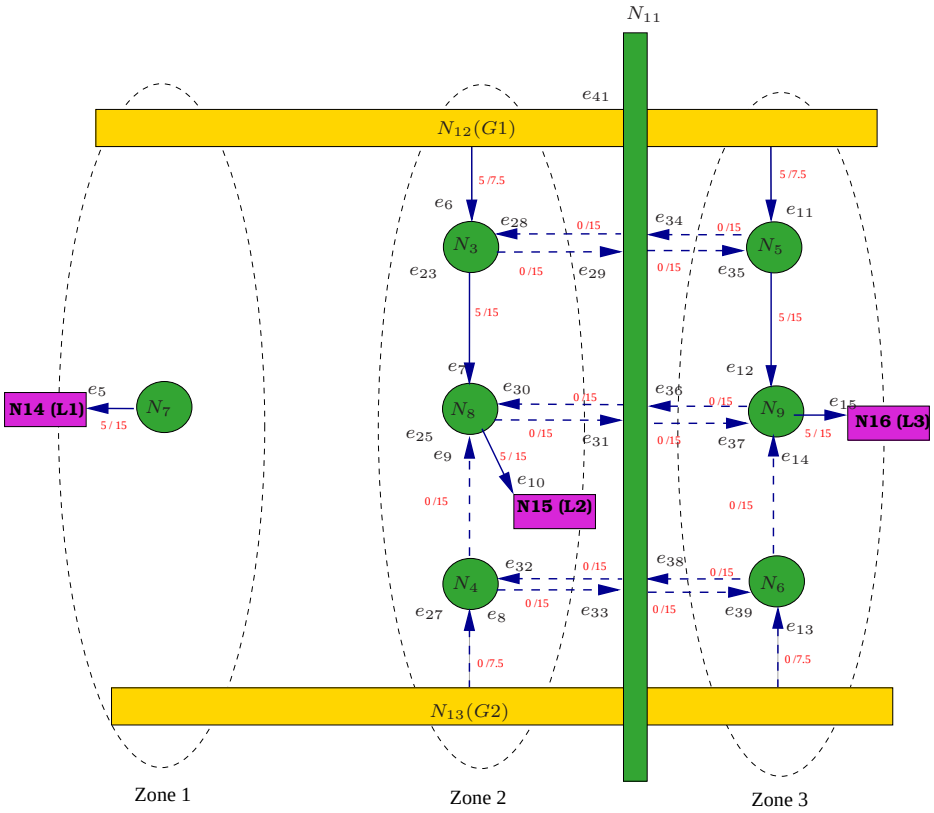

Figure 5–4: Full DCZEDS with faults on N_1, N_2 and N_{10}

After isolation of the nodes N_1, N_2 and N_{10}, the edge-status vector and edge-flux vector were updated as shown in Table 5–18 and 5–19 respectively.

As a result of these three faults, the system presents unbalance on node N_7 as shown in Table 5–20. In this case, the algorithm tries to reach the unbalanced node but the node is unreachable because there are not paths that can connect it to a source.

Table 5–18: Updated Edge-Status vector after isolation of nodes N_1, N_2 and N_{10} on the full DCZEDS.

Edge	e_1	e_2	e_3	e_4	e_5	e_6	e_7	e_8	e_9	e_{10}	e_{11}	e_{12}	e_{13}	e_{14}	e_{15}	e_{16}	e_{17}	e_{18}	e_{19}	e_{20}	e_{21}	e_{22}	e_{23}	e_{24}	e_{25}	e_{26}	e_{27}	e_{28}	e_{29}	e_{30}	e_{31}	e_{32}	e_{33}	e_{34}	e_{35}	e_{36}	e_{37}	e_{38}	e_{39}	e_{40}	e_{41}
$\boldsymbol{Y_s}$	0	0	0	0	1	1	1	0	0	1	1	1	0	0	1	0	0	0	0	0	0	0	0	0	0	0	0	0	0	0	0	0	0	0	0	0	0	0	0

Table 5–19: Updated Edge-Flux vector after isolation of nodes N_1, N_2 and N_{10} on the full DCZEDS.

Edge	e_5	e_6	e_7	e_8	e_9	e_{10}	e_{11}	e_{12}	e_{13}	e_{14}	e_{15}	e_{28}	e_{29}	e_{30}	e_{31}	e_{32}	e_{33}	e_{34}	e_{35}	e_{36}	e_{37}	e_{38}	e_{39}
$\boldsymbol{F(KW)}$	5	5	5	0	0	5	5	5	0	0	5	0	0	0	0	0	0	0	0	0	0	0	0

Table 5–20: Updated Node-Power vector updated after isolation of N_1, N_2 and N_{10} on the full DCZEDS.

Node	N_3	N_4	N_5	N_6	N_7	N_8	N_9	N_{11}	N_{12}	N_{13}	N_{14}	N_{15}	N_{16}
Net Power (KW)	0	0	0	0	-5	0	0	0	-10	0	5	5	5

To avoid the unbalance in the system, it is necessary to shed load L_1. The algorithm identifies that edge e_5 is the only one that needs to be disconnected and the new edge-status vector, edge-flux vector, and power on each node are calculated, see Tables 5–21, 5–22 and 5–23 respectively. The updated graph is shown in Figure 5–5.

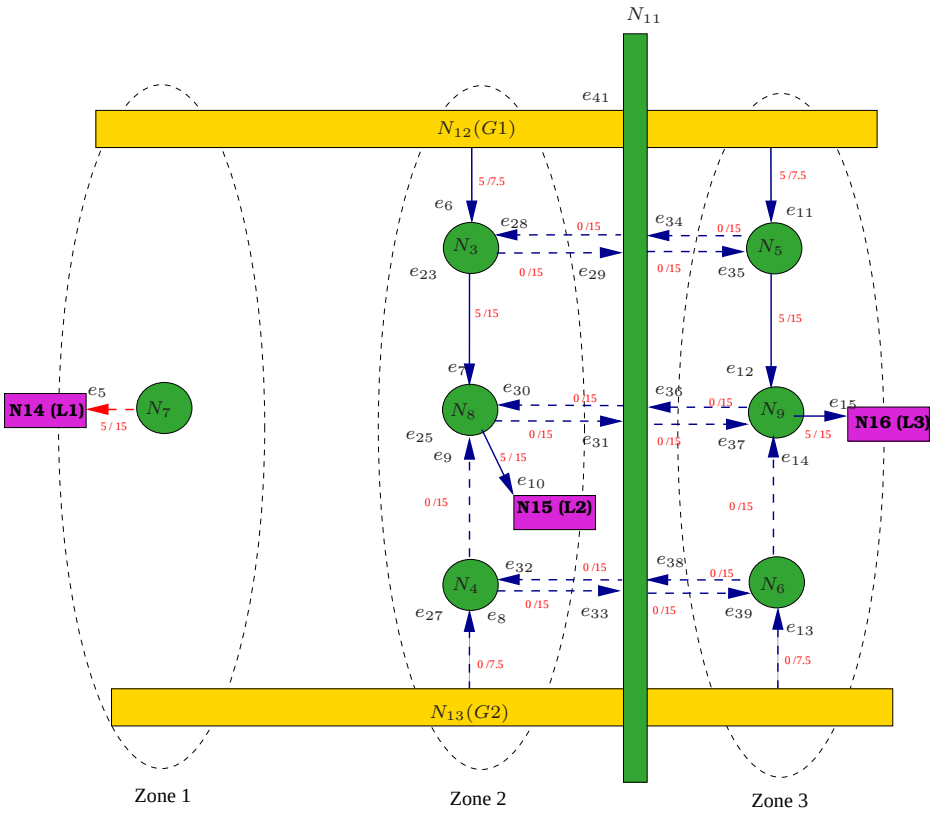

Figure 5–5: Full DCZEDS with isolation of L_1.

Table 5–21: Updated Edge-Status vector after isolation of load L_1 on the full DCZEDS.

Edge	e_1	e_2	e_3	e_4	e_5	e_6	e_7	e_8	e_9	e_{10}	e_{11}	e_{12}	e_{13}	e_{14}	e_{15}	e_{16}	e_{17}	e_{18}	e_{19}	e_{20}	e_{21}	e_{22}	e_{23}	e_{24}	e_{25}	e_{26}	e_{27}	e_{28}	e_{29}	e_{30}	e_{31}	e_{32}	e_{33}	e_{34}	e_{35}	e_{36}	e_{37}	e_{38}	e_{39}	e_{40}	e_{41}
$\boldsymbol{Y_s}$	0	0	0	0	0	1	1	0	0	1	1	1	0	0	1	0	0	0	0	0	0	0	0	0	0	0	0	0	0	0	0	0	0	0	0	0	0	0	0

Table 5–22: Updated Edge-Flux vector after isolation of load L_1 on the full DCZEDS.

Edge	e_5	e_6	e_7	e_8	e_9	e_{10}	e_{11}	e_{12}	e_{13}	e_{14}	e_{15}	e_{28}	e_{29}	e_{30}	e_{31}	e_{32}	e_{33}	e_{34}	e_{35}	e_{36}	e_{37}	e_{38}	e_{39}
$\boldsymbol{F(KW)}$	0	5	5	0	0	5	5	5	0	0	5	0	0	0	0	0	0	0	0	0	0	0	0

Table 5–23: Updated Node-Power vector updated after isolation of load L_1 on the full DCZEDS.

Node	N_3	N_4	N_5	N_6	N_7	N_8	N_9	N_{11}	N_{12}	N_{13}	N_{14}	N_{15}	N_{16}
Net Power (KW)	0	0	0	0	0	0	0	0	-10	0	0	5	5

5.3.2 Simultaneous faults

The second scenario for the full DCZEDS, in this case there are simultaneously faults on nodes N_1 and N_2 and at the same time the load power demand on L_1 (N_{14}) is increased to $13KW$. The reconfiguration algorithm redistributed the power flow on all the system tracing different paths to balance it.

The starting point for this example is the DCZEDS showed in Figure 5–3. The edges to be tripped to isolate the nodes N_1 and N_2 are shown in Table 5–24 and its graph representation in Figure 5–6.

Table 5–24: Edge tripped to isolate N_1 and N_2 on the full DCZEDS.

Edges Tripped	[1	2	3	4	16	17	20	21]

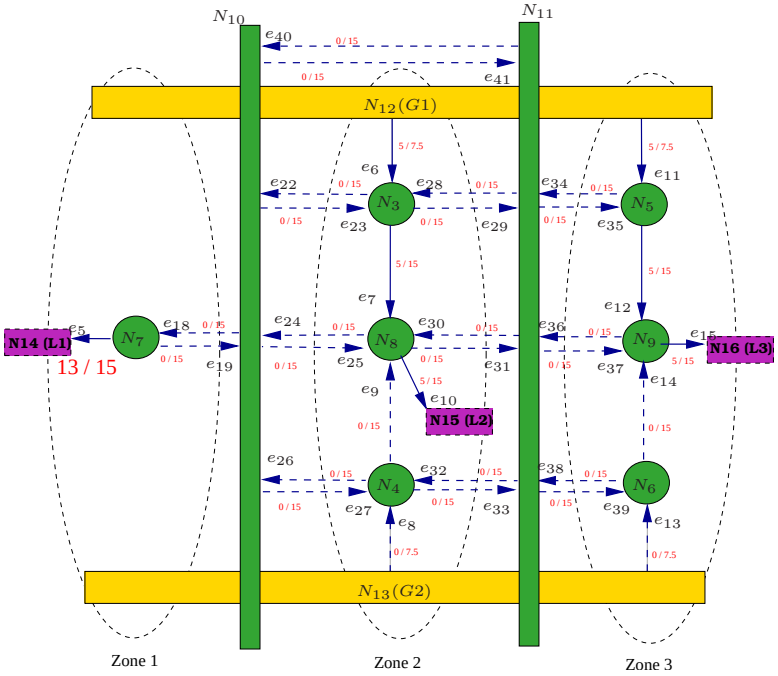

Figure 5–6: Full DCZEDS with fault on N_1, N_2 and increment on load L_1.

After isolation of node N_1 and N_2 and the increment on L_1, the edge-flux vector, edge-status vector, and the net power on each node were updated as shown in Tables 5–25, 5–26, and 5–27.

Table 5–25: Updated Edge-Status vector after isolation of nodes N_1 and N_2 and increment on load L_1, on the full DCZEDS.

Edge	e_1	e_2	e_3	e_4	e_5	e_6	e_7	e_8	e_9	e_{10}	e_{11}	e_{12}	e_{13}	e_{14}	e_{15}	e_{16}	e_{17}	e_{18}	e_{19}	e_{20}	e_{21}	e_{22}	e_{23}	e_{24}	e_{25}	e_{26}	e_{27}	e_{28}	e_{29}	e_{30}	e_{31}	e_{32}	e_{33}	e_{34}	e_{35}	e_{36}	e_{37}	e_{38}	e_{39}	e_{40}	e_{41}
$\boldsymbol{Y_s}$	0	0	0	0	1	1	1	0	0	1	1	1	0	0	1	0	0	0	0	0	0	0	0	0	0	0	0	0	0	0	0	0	0	0	0	0	0	0	0	0

Table 5–26: Updated Edge-Flux vector after isolation of nodes N_1 and N_2 and increment on L_1, on the full DCZEDS.

Edge	e_3	e_4	e_5	e_6	e_7	e_8	e_9	e_{10}	e_{11}	e_{12}	e_{13}	e_{14}	e_{15}	e_{18}	e_{19}	e_{20}	e_{21}	e_{22}	e_{23}	e_{24}	e_{25}	e_{26}	e_{27}	e_{28}	e_{29}	e_{30}	e_{31}	e_{32}	e_{33}	e_{34}	e_{35}	e_{36}	e_{37}	e_{38}	e_{39}	e_{40}	e_{41}
$\boldsymbol{F(KW)}$	0	0	13	5	5	0	0	5	5	5	0	0	5	0	0	0	0	0	0	0	0	0	0	0	0	0	0	0	0	0	0	0	0	0	0	0	0	0	0	0

Table 5–27: Updated Node-Power vector updated after isolation of N_1 and N_2 and increment on L_1 on the full DCZEDS.

Node	N_3	N_4	N_5	N_6	N_7	N_8	N_9	N_{10}	N_{11}	N_{12}	N_{13}	N_{14}	N_{15}	N_{16}
Net Power (KW)	0	0	0	0	-13	0	0	0	0	-10	0	13	5	5

The system presents an unbalance on N_7 of $13KW$. The algorithm first extracts the maximum capacity of the SSCM connected to main bus of the zone 2 (N_3), which is $7.5KW$, but there is still an unbalance of $5.5KW$ on N_7. Then, the algorithm finds other path to meet the load power demand, which connect the alternate SSCM N_4 of the adjacent zone. The paths to connect the zones are shown in Table 5–28 and their graph representation is shown in Figure 5–7. The updated matrices after this reconfiguration are shown in Tables 5–29,5–30 and 5–31.

Table 5–28: Paths selected to balance N_7 after simultaneous faults occurred

From N_3		From N_4	
Edges	Nodes	Edges	Nodes
[18 22]	[7 10 3]	[18 26]	[7 10 4]

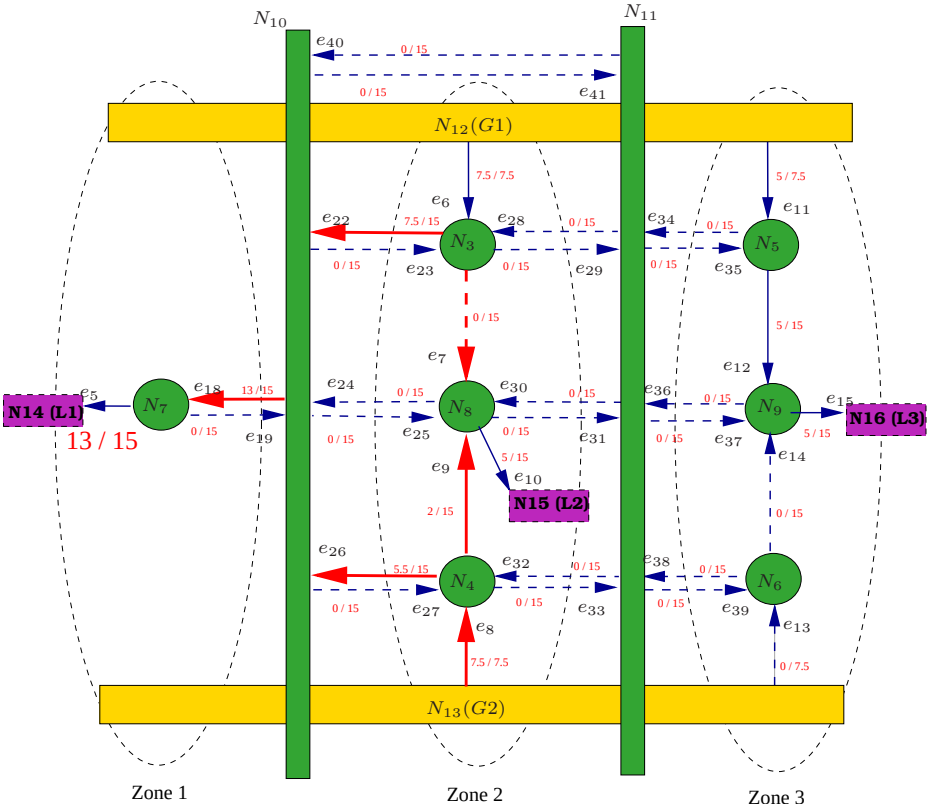

Figure 5–7: Full DCZEDS with N_7 balanced after fault detection on N_1 and N_2, and increment on L_1

Table 5–29: Updated Edge-Status vector with N_7 balanced after simultaneous faults occurred.

Edge	e_1	e_2	e_3	e_4	e_5	e_6	e_7	e_8	e_9	e_{10}	e_{11}	e_{12}	e_{13}	e_{14}	e_{15}	e_{16}	e_{17}	e_{18}	e_{19}	e_{20}	e_{21}	e_{22}	e_{23}	e_{24}	e_{25}	e_{26}	e_{27}	e_{28}	e_{29}	e_{30}	e_{31}	e_{32}	e_{33}	e_{34}	e_{35}	e_{36}	e_{37}	e_{38}	e_{39}	e_{40}	e_{41}
Y_s	0	0	0	0	1	1	0	1	1	1	1	1	0	0	1	0	0	1	0	0	0	1	0	0	0	1	0	0	0	0	0	0	0	0	0	0	0	0	0	0

Table 5–30: Updated Edge-Flux vector with N_7 balanced after simultaneous faults occurred.

Edge	e_3	e_4	e_5	e_6	e_7	e_8	e_9	e_{10}	e_{11}	e_{12}	e_{13}	e_{14}	e_{15}	e_{18}	e_{19}	e_{20}	e_{21}	e_{22}	e_{23}	e_{24}	e_{25}	e_{26}	e_{27}	e_{28}	e_{29}	e_{30}	e_{31}	e_{32}	e_{33}	e_{34}	e_{35}	e_{36}	e_{37}	e_{38}	e_{39}	e_{40}	e_{41}
$F(KW)$	0	0	13	7.5	0	7.5	2	5	5	5	0	0	5	13	0	0	0	7.5	0	0	0	5.5	0	0	0	0	0	0	0	0	0	0	0	0	0	0	0	0	0

Table 5–31: Updated Node-Power vector with N_7 balanced after simultaneous faults occurred.

Node	N_3	N_4	N_5	N_6	N_7	N_8	N_9	N_{10}	N_{11}	N_{12}	N_{13}	N_{14}	N_{15}	N_{16}
Net Power (KW)	0	0	0	0	0	-3	0	0	0	-12.5	-7.5	13	5	5

Here, it is important to observe that the node N_7 was balanced, but this caused an unbalance of $3KW$ on N_8, which represents that the power demand of load 2 is not supplied. This occurred because the load 2 has less priority than load 1. However, the algorithm found that the system has enough capacity to feed the load L_2 and also verified that this load is reachable. Then, the path selected to balance N_8 is shown in Table 5–32 and it is observed in Figure 5–8. The status, flow and power, were updated and are shown in Tables 5–33, 5–34 and 5–35 respectively.

Table 5–32: Path selected to balance N_8 after N_7 was balanced

From N_5	
Edges	Nodes
[30 34]	[8 11 5]

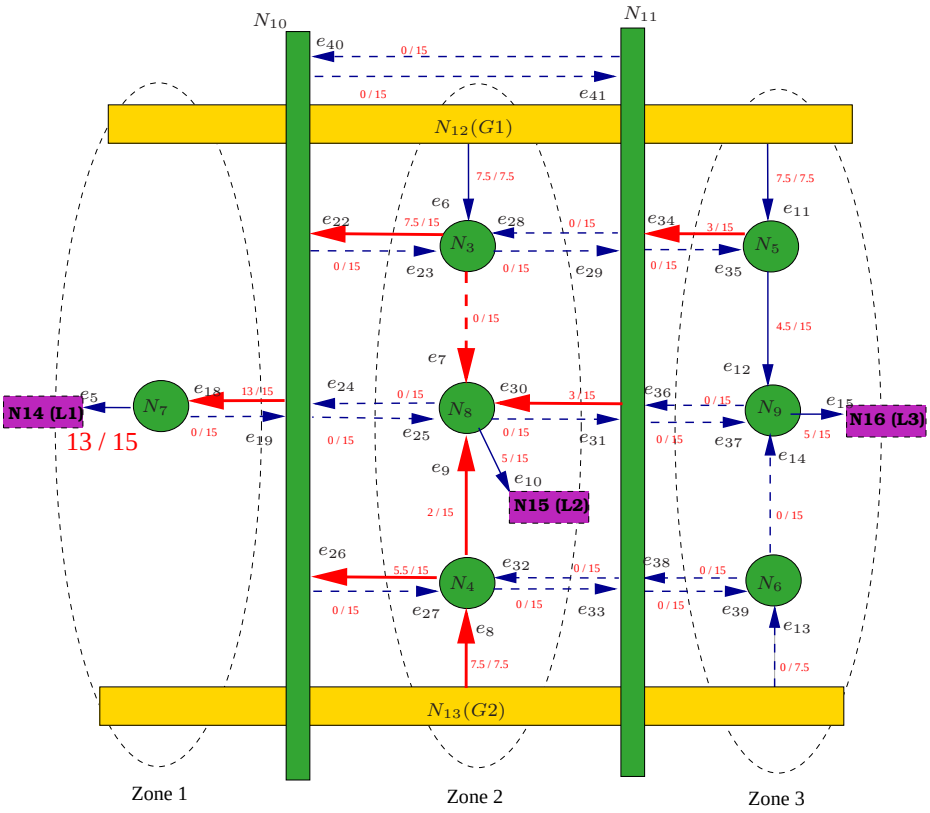

Figure 5–8: Full DCZEDS with nodes N_7 and N_8 balanced.

Table 5–33: Updated Edge-Status vector with N_8 and N_7 balanced.

Edge	e_1	e_2	e_3	e_4	e_5	e_6	e_7	e_8	e_9	e_{10}	e_{11}	e_{12}	e_{13}	e_{14}	e_{15}	e_{16}	e_{17}	e_{18}	e_{19}	e_{20}	e_{21}	e_{22}	e_{23}	e_{24}	e_{25}	e_{26}	e_{27}	e_{28}	e_{29}	e_{30}	e_{31}	e_{32}	e_{33}	e_{34}	e_{35}	e_{36}	e_{37}	e_{38}	e_{39}	e_{40}	e_{41}
$\boldsymbol{Y_s}$	0	0	0	0	1	1	0	1	1	1	1	1	0	0	1	0	0	1	0	0	0	1	0	0	0	1	0	0	0	1	0	0	0	1	0	0	0	0	0	0

Table 5–34: Updated Edge-Flux vector with N_8 and N_7 balanced.

Edge	e_3	e_4	e_5	e_6	e_7	e_8	e_9	e_{10}	e_{11}	e_{12}	e_{13}	e_{14}	e_{15}	e_{18}	e_{19}	e_{20}	e_{21}	e_{22}	e_{23}	e_{24}	e_{25}	e_{26}	e_{27}	e_{28}	e_{29}	e_{30}	e_{31}	e_{32}	e_{33}	e_{34}	e_{35}	e_{36}	e_{37}	e_{38}	e_{39}	e_{40}	e_{41}
$\boldsymbol{F(KW)}$	0	0	13	7.5	0	7.5	2	5	7.5	4.5	0	0	5	13	0	0	0	7.5	0	0	0	5.5	0	0	0	3	0	0	0	3	0	0	0	0	0	0	0	0	0

Table 5–35: Updated Node-Power vector with N_8 and N_7 balanced.

Node	N_3	N_4	N_5	N_6	N_7	N_8	N_9	N_{10}	N_{11}	N_{12}	N_{13}	N_{14}	N_{15}	N_{16}
Net Power (KW)	0	0	0	0	0	0	-0.5	0	0	-15	-7.5	13	5	5

After N_8 was balanced, there is an unbalance on node N_9 of $0.5KW$, in this case the load 3 cannot be completely supplied. Then, the algorithm detects that it is possible to switch the auctioneering diodes into the zone 3 to balance N_9, taking the total power to supply the load 3 from N_6. The updated matrices are shown in tables 5–36, 5–37 and 5–38 respectively. The power flow through the converter connected to the main bus into the zone 3, was reduced because only supplies the load into the zone 2.

At this point, the algorithm found that power is balanced in all nodes and the reconfiguration process is ended.

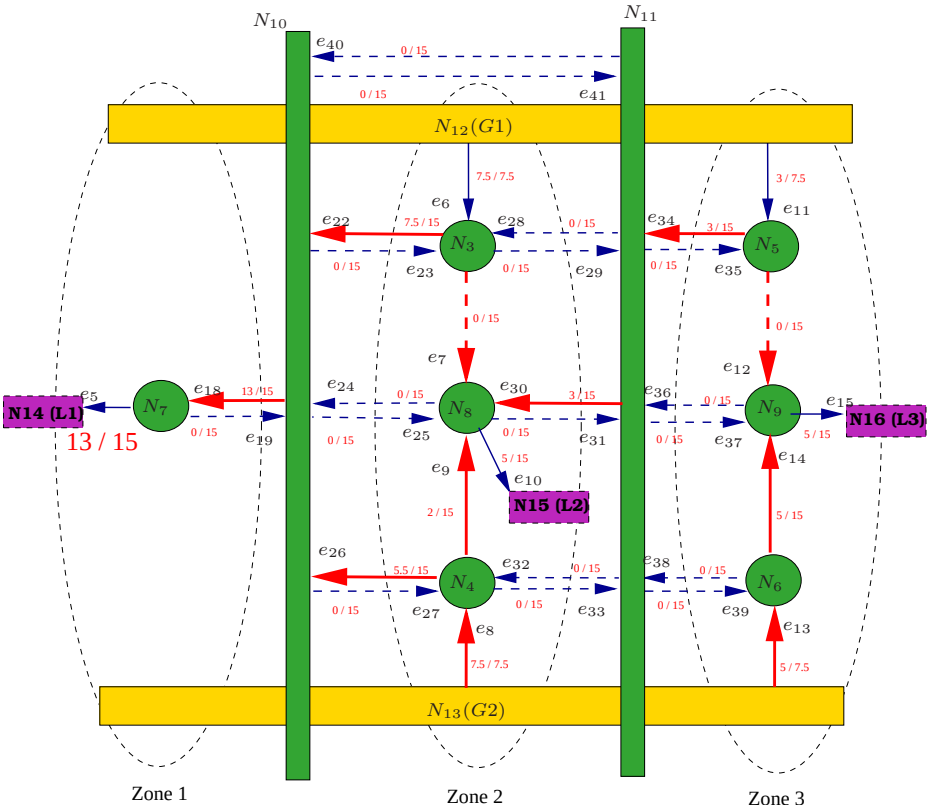

Figure 5–9: Full DCZEDS with nodes N_7 and N_8 balanced

Table 5–36: Updated Edge-Status vector with N_9 balanced.

Edge	e_1	e_2	e_3	e_4	e_5	e_6	e_7	e_8	e_9	e_{10}	e_{11}	e_{12}	e_{13}	e_{14}	e_{15}	e_{16}	e_{17}	e_{18}	e_{19}	e_{20}	e_{21}	e_{22}	e_{23}	e_{24}	e_{25}	e_{26}	e_{27}	e_{28}	e_{29}	e_{30}	e_{31}	e_{32}	e_{33}	e_{34}	e_{35}	e_{36}	e_{37}	e_{38}	e_{39}	e_{40}	e_{41}
Y_s	0	0	0	0	1	1	0	1	1	1	1	0	1	1	1	0	0	1	0	0	0	1	0	0	0	1	0	0	0	1	0	0	0	1	0	0	0	0	0	0

Table 5–37: Updated Edge-Flux vector with N_9 balanced.

Edge	e_3	e_4	e_5	e_6	e_7	e_8	e_9	e_{10}	e_{11}	e_{12}	e_{13}	e_{14}	e_{15}	e_{18}	e_{19}	e_{20}	e_{21}	e_{22}	e_{23}	e_{24}	e_{25}	e_{26}	e_{27}	e_{28}	e_{29}	e_{30}	e_{31}	e_{32}	e_{33}	e_{34}	e_{35}	e_{36}	e_{37}	e_{38}	e_{39}	e_{40}	e_{41}
$F(KW)$	0	0	13	7.5	0	7.5	2	5	3	0	5	5	5	13	0	0	0	7.5	0	0	0	5.5	0	0	0	3	0	0	0	3	0	0	0	0	0	0	0	0

Table 5–38: Updated Node-Power Matrix with N_9 balanced.

Node	N_3	N_4	N_5	N_6	N_7	N_8	N_9	N_{10}	N_{11}	N_{12}	N_{13}	N_{14}	N_{15}	N_{16}
Net Power (KW)	0	0	0	0	0	0	0	0	0	-10.5	-12.5	13	5	5

5.3.3 Load Restoration

This scenario is assumed starting from the last reconfigured system (Figure 5–9). Now, there is a fault on the main SSCM in the zone 3 (N_5), the edges tripped to isolate the fault node are shown in Table 5–39. The current system graph is shown in Figure 5–10 and the updated matrices are shown in Tables 5–40, 5–41 and 5–42. As you can see, the power that can be given to L_2 is not enough to supply all of their power demand, and N_8 is again unbalanced.

Table 5–39: Edge tripped to isolate N_5 on full DCZEDS.

Edges Tripped	[11 12 34 35]

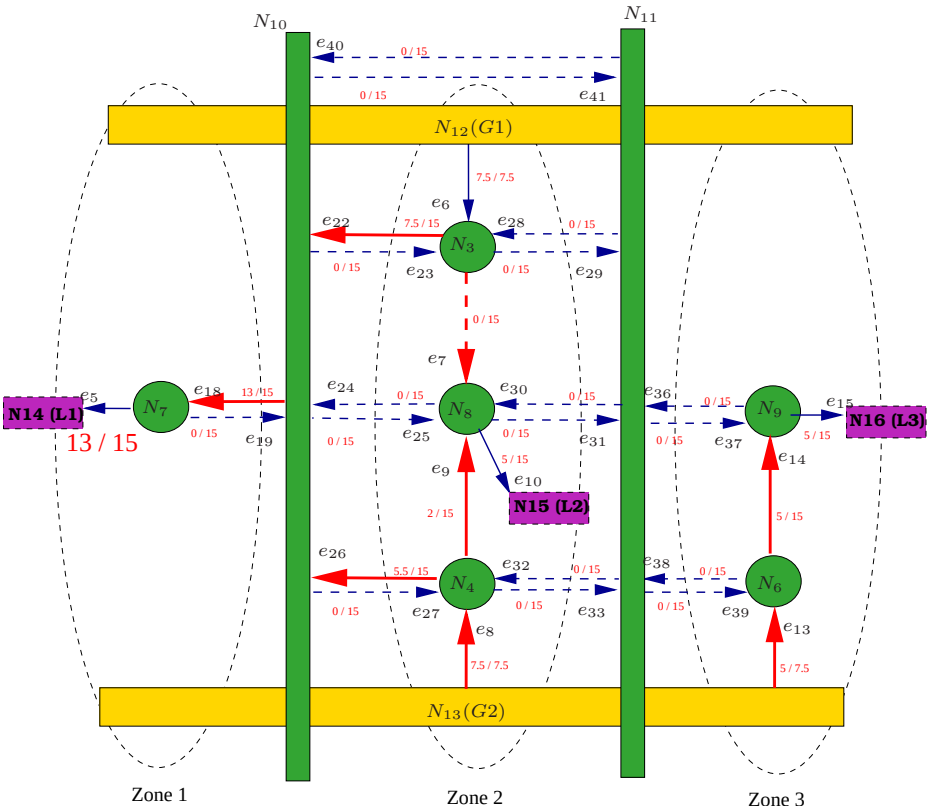

Figure 5–10: Full DCZEDS with N_5 isolated.

Table 5–40: Updated Edge-Status vector after isolation on node N_5.

Edge	e_1	e_2	e_3	e_4	e_5	e_6	e_7	e_8	e_9	e_{10}	e_{11}	e_{12}	e_{13}	e_{14}	e_{15}	e_{16}	e_{17}	e_{18}	e_{19}	e_{20}	e_{21}	e_{22}	e_{23}	e_{24}	e_{25}	e_{26}	e_{27}	e_{28}	e_{29}	e_{30}	e_{31}	e_{32}	e_{33}	e_{34}	e_{35}	e_{36}	e_{37}	e_{38}	e_{39}	e_{40}	e_{41}
$\boldsymbol{Y_s}$	0	0	0	0	1	1	0	1	1	1	0	0	1	1	1	0	0	1	0	0	0	1	0	0	0	1	0	0	0	1	0	0	0	0	0	0	0	0	0	0

Table 5–41: Updated Edge-Flux vector after isolation on node N_5.

Edge	e_3	e_4	e_5	e_6	e_7	e_8	e_9	e_{10}	e_{13}	e_{14}	e_{15}	e_{18}	e_{19}	e_{20}	e_{21}	e_{22}	e_{23}	e_{24}	e_{25}	e_{26}	e_{27}	e_{28}	e_{29}	e_{30}	e_{31}	e_{32}	e_{33}	e_{36}	e_{37}	e_{38}	e_{39}	e_{40}	e_{41}
$\boldsymbol{F(KW)}$	0	0	13	7.5	0	7.5	2	5	5	5	5	13	0	0	0	7.5	0	0	0	5.5	0	0	0	0	0	0	0	0	0	0	0	0

Table 5–42: Updated Node-Power Matrix after isolation on node N_5.

Node	N_3	N_4	N_6	N_7	N_8	N_9	N_{10}	N_{11}	N_{12}	N_{13}	N_{14}	N_{15}	N_{16}
Net Power (KW)	0	0	0	0	-3	0	0	0	-7.5	-12.5	13	5	5

In this case, the lower priority load (L_3) is supplied instead of load with a higher priority (L_2). The algorithm found that the total system capacity ($22.5KW$) is less that the loads power demand ($23KW$)and then the lower priority load must be shed. To do this, first it is disconnected the path that is actually supplying the L_3 and then the flow are updating on over the graph. After, a new path is founded to balance the N_8, see Table 5–43 and Figure 5–11. The reconfiguration process ends in this point and the updated vectors are shown in Tables 5–44, 5–45 and 5–46.

Table 5–43: Path selected to balance N_8 after isolation of N_5

From N_6	
Edges	Nodes
[30 38]	[8 11 6]

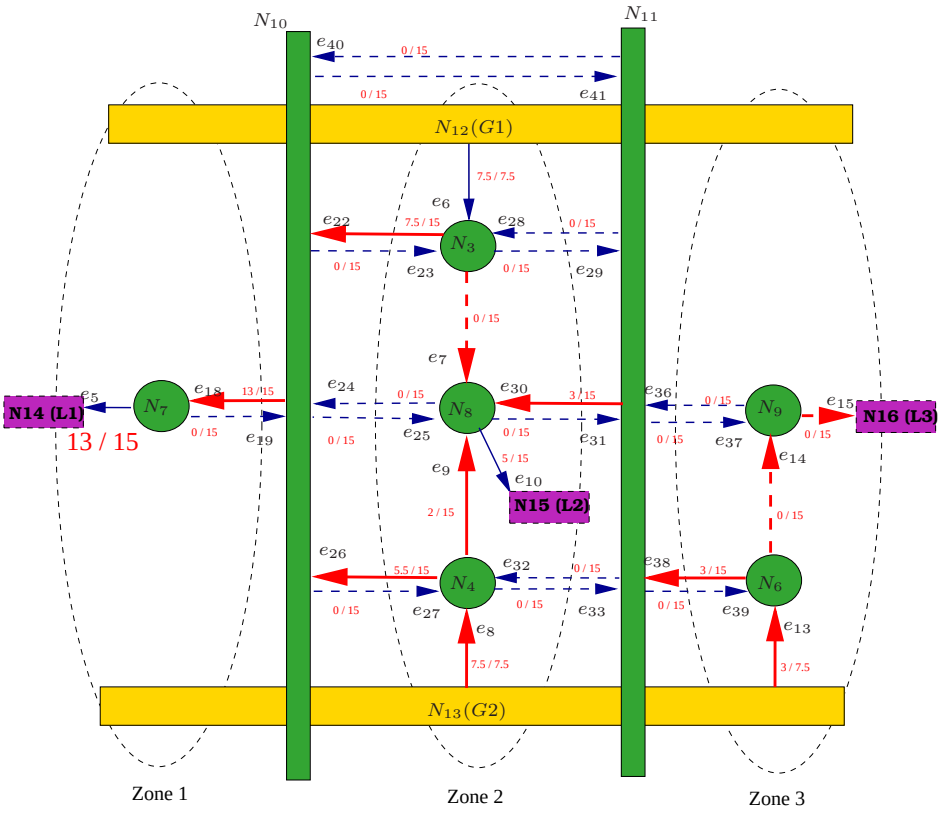

Figure 5–11: Full DCZEDS with path to balance N_8 after isolation of N_5

Table 5–44: Updated Edge-Status vector with N_8 balanced after fault on N_5

Edge	e_1	e_2	e_3	e_4	e_5	e_6	e_7	e_8	e_9	e_{10}	e_{11}	e_{12}	e_{13}	e_{14}	e_{15}	e_{16}	e_{17}	e_{18}	e_{19}	e_{20}	e_{21}	e_{22}	e_{23}	e_{24}	e_{25}	e_{26}	e_{27}	e_{28}	e_{29}	e_{30}	e_{31}	e_{32}	e_{33}	e_{34}	e_{35}	e_{36}	e_{37}	e_{38}	e_{39}	e_{40}	e_{41}
$\boldsymbol{Y_s}$	0	0	0	0	1	1	0	1	1	1	0	0	1	0	0	0	0	1	0	0	0	1	0	0	0	1	0	0	0	1	0	0	0	0	0	0	0	1	0	0	0

Table 5–45: Updated Edge-Flux vector with N_8 balanced after fault on N_5

Edge	e_3	e_4	e_5	e_6	e_7	e_8	e_9	e_{10}	e_{13}	e_{14}	e_{15}	e_{18}	e_{19}	e_{20}	e_{21}	e_{22}	e_{23}	e_{24}	e_{25}	e_{26}	e_{27}	e_{28}	e_{29}	e_{30}	e_{31}	e_{32}	e_{33}	e_{36}	e_{37}	e_{38}	e_{39}	e_{40}	e_{41}
$\boldsymbol{F(KW)}$	0	0	13	7.5	0	7.5	2	5	3	0	0	13	0	0	0	7.5	0	0	0	5.5	0	0	0	0	0	3	0	0	3	0	0	0

Table 5–46: Updated Node-Power Matrix with N_8 balanced after fault on N_5

Node	N_3	N_4	N_6	N_7	N_8	N_9	N_{10}	N_{11}	N_{12}	N_{13}	N_{14}	N_{15}	N_{16}
Net Power (KW)	0	0	0	0	0	0	0	0	-7.5	-10.5	13	5	0

Now, the power demand of load 3 is reduced to $3KW$, the algorithm detected this change and found that system has enough capacity to feed the three loads, but at the moment one of these is shed and needs to be restored. In this case, this power demand can be extracted from the alternate converter into the zone 3, see Figure 5–12. The system is balanced and the process ends because the system constraints are satisfied, see Tables 5–47, 5–48 and 5–49.

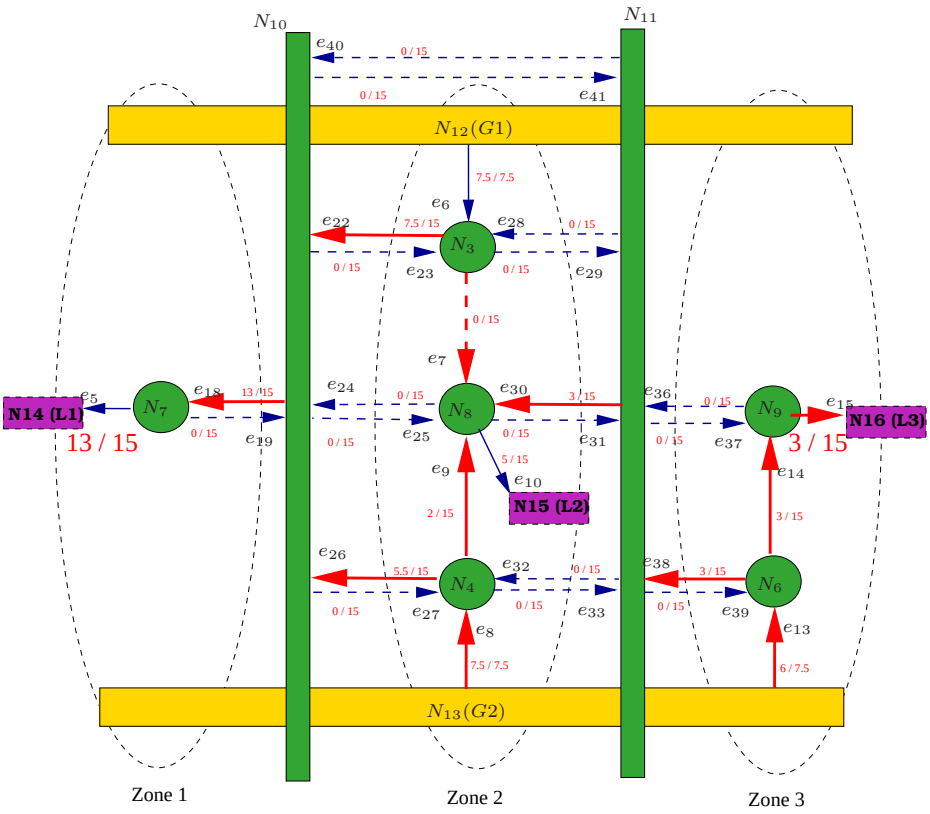

Figure 5–12: Full DCZEDS with restoration of L_3.

Table 5–47: Updated Edge-Status vector with L_3 restored.

Edge	e_1	e_2	e_3	e_4	e_5	e_6	e_7	e_8	e_9	e_{10}	e_{11}	e_{12}	e_{13}	e_{14}	e_{15}	e_{16}	e_{17}	e_{18}	e_{19}	e_{20}	e_{21}	e_{22}	e_{23}	e_{24}	e_{25}	e_{26}	e_{27}	e_{28}	e_{29}	e_{30}	e_{31}	e_{32}	e_{33}	e_{34}	e_{35}	e_{36}	e_{37}	e_{38}	e_{39}	e_{40}	e_{41}
Y_s	0	0	0	0	1	1	0	1	1	1	0	0	1	1	1	0	0	1	0	0	0	1	0	0	0	1	0	0	0	1	0	0	0	0	0	0	0	1	0	0	0

Table 5–48: Updated Edge-Flux vector updated with L_3 restored.

Edge	e_3	e_4	e_5	e_6	e_7	e_8	e_9	e_{10}	e_{13}	e_{14}	e_{15}	e_{18}	e_{19}	e_{20}	e_{21}	e_{22}	e_{23}	e_{24}	e_{25}	e_{26}	e_{27}	e_{28}	e_{29}	e_{30}	e_{31}	e_{32}	e_{33}	e_{36}	e_{37}	e_{38}	e_{39}	e_{40}	e_{41}
$F(KW)$	0	0	13	7.5	0	7.5	2	5	6	3	3	13	0	0	0	7.5	0	0	0	5.5	0	0	0	0	0	3	0	0	3	0	0	0

Table 5–49: Updated Node-Power Matrix with L_3 restored.

Node	N_3	N_4	N_6	N_7	N_8	N_9	N_{10}	N_{11}	N_{12}	N_{13}	N_{14}	N_{15}	N_{16}
Net Power (KW)	0	0	0	0	0	0	0	0	-7.5	-13.5	13	5	3

5.4 Summary

Some scenarios were tested on the DC Zonal Electric Distribution System (single and full) explained in Chapter 4. The effectiveness of the reconfiguration algorithm proposed was demonstrated because was possible to shed loads with lower priority in both systems, and to shed load when was unreachable in the full DCZEDS. Also, it reconfigured the system when simultaneous faults occurred together with an increment of power demand on the higher priority load. And by last, one case of load restoration was shown.

All of the topologies obtained after the reconfiguration process were the expected in each scenario, since always the loads with higher priority were the first restored with exception of the second scenario, where the load with higher priority was disconnected because it was unreachable.

CHAPTER 6
Conclusions and Future Work

6.1 Conclusions

The study and application of graph theory to develop a reconfiguration algorithm on DC Zonal Electric Distribution Systems was presented in this thesis. This kind of systems has unique system architectures, characteristics, dynamics and stability problems which are not similar to those of conventional AC electrical power distribution systems. These systems also need to be reconfigured quickly after a fault event occurs.

The reconfiguration of DCZEDS was posed as a network flow multi-objective optimization problem, where we maximized the number of served high priority loads and minimized the switching operations needed to realize the new topology. The system constraints also were included in the optimization problem to ensure safe operating conditions.

The reconfiguration algorithm was implemented in Matlab and maximized the number of high priority loads by efficient manipulation of the matrix representation of the system, derived from its graph representation (e.g. Incidence matrix, switch status matrix, instantaneous power flow matrix).

Also, the reconfiguration algorithm was developed under the methodology of [25] (Figure 2–4), where the process can run repeatedly and solve the problem in a centralized manner. Under this scheme, each time the process began, the algorithm acquired the updated system data, and in this way the loads were reconfigured with the current load power demand. In other words, the algorithm was capable to reconfigure variable loads analyzing the residual capacity of the network at the moment of fault.

Some scenarios were tested with the ONR DC Zonal Electric Distribution System to verify the performance of the algorithm. These results showed the reconfiguration process when it was necessary to shed loads because of unreachability and low priority. Also, scenarios were presented in which the loads power demand were increased and decreased. In each case, the algorithm found the necessary path to reconfigure the system solving the proposed optimization problem.

Besides, other DC power distribution systems were studied to verify the generality of the reconfiguration algorithm, the study only carried out the graph representation of the system. The matrices for each system can be constructed in the same manner than in the example presented in Chapter 4.

Finally, it is possible to say that the algorithm has the capacity to isolate faults nodes, feed the loads with higher priority, shed or pick-up loads under different situations and also reconfigures systems with variable loads.

6.2 Future Work

- Future work includes to simulate a test system and to develop an interface between protecting devices and the Matlab functions that establish the protection setting required.

- Also, we recommend to develop a reconfiguration process based on distributed control where each controller in the system uses the reconfiguration algorithm presented in this thesis (e.g. high reliability distribution system HRDS in Section 4.5.1).

- Generally, the real systems developed have storage elements to supply at some of the loads. For this reason it is needed to add this kind of elements into the reconfiguration algorithm. It is important to keep in mind that the storage elements, such as UPS (Uninterruptible Power Supply) or batteries, can be considered as generators or loads, depending of the power demand.

BIBLIOGRAPHY

[1] M. E. Ali Emadi and J. Miller, *Vehicular Electric Power System.* Marcel Dekker, Inc., 2004.

[2] O. Amoda and N. Schulz, "An adaptive protection scheme for shipboard power systems," *Electric Ship Technologies Symposium, 2007. ESTS '07. IEEE*, pp. 225–230, May 2007.

[3] J. Amy, J.V., "Considerations in the design of naval electric power systems," *Power Engineering Society Summer Meeting, 2002 IEEE*, vol. 1, pp. 331–335 vol.1, 25-25 July 2002.

[4] G. Antonoiu and P. K. Srimani, "Distributed self-stabilizing algorithm for minimum spanning tree construction," in *Euro-Par '97: Proceedings of the Third International Euro-Par Conference on Parallel Processing.* London, UK: Springer-Verlag, 1997, pp. 480–487.

[5] K. Aoki, H. Kuwabara, T. Satoh, and M. Kanezashi, "Outage state optimal load allocation by automatic sectionalizing switches operation in distribution systems," *Power Delivery, IEEE Transactions on*, vol. 2, no. 4, pp. 1177–1185, Oct. 1987.

[6] T. Baldwin and S. Lewis, "Distribution load flow methods for shipboard power systems," *Industry Applications, IEEE Transactions on*, vol. 40, no. 5, pp. 1183–1190, Oct 2004.

[7] M. L. Balinski and R. E. Gomory, "A primal method for the assignment and transportation problems," *Management Science*, vol. 10, no. 3, pp. 578–593, 1964.

[8] M. Baran and N. Mahajan, "Dc distribution for industrial systems: opportunities and challenges," *Industrial and Commerical Power Systems Technical Conference, 2002. 2002 IEEE*, pp. 38–41, 8-8 May 2002.

[9] M. Baran, S. Teleke, and S. Bhattacharya, "Overcurrent protection in dc zonal shipboard power systems using solid state protection devices," *Electric Ship Technologies Symposium, 2007. ESTS '07. IEEE*, pp. 221–224, 21-23 May 2007.

[10] K. L. Butler, N. D. R. Sarma, and V. Ragendra Prasad, "Network reconfiguration for service restoration in shipboard power distribution systems," *Power Engineering Review, IEEE*, vol. 21, no. 11, pp. 55–55, Nov. 2001.

[11] K. Butler and N. Sarma, "General reconfiguration methodology for ac radial shipboard power systems," *Power Engineering Society Winter Meeting, 2000. IEEE*, vol. 2, pp. 1226–1230 vol.2, 2000.

[12] K. Butler, N. Sarma, and V. Ragendra Prasad, "Network reconfiguration for service restoration in shipboard power distribution systems," *Power Engineering Society Winter Meeting, 2002. IEEE*, vol. 2, pp. 870 vol.2–, 2002.

[13] K. Butler, N. Sarma, C. Whitcomb, H. Do Carmo, and H. Zhang, "Shipboard systems deploy automated protection," *Computer Applications in Power, IEEE*, vol. 11, no. 2, pp. 31–36, Apr 1998.

[14] K. Butler-Purry and N. Sarma, "Self-healing reconfiguration for restoration of naval shipboard power systems," *Power Systems, IEEE Transactions on*, vol. 19, no. 2, pp. 754–762, May 2004.

[15] D. B. Campbell, "Electric power distribution systems operations," Naval Facilities Engineering Command, Tech. Rep., 1990.

[16] S.-K. Chai and A. Sekar, "Graph theory application to deregulated power system," *System Theory, 2001. Proceedings of the 33rd Southeastern Symposium on*, pp. 117–121, Mar 2001.

[17] J. Ciezki and R. Ashton, "Selection and stability issues associated with a navy shipboard dc zonal electric distribution system," *Power Delivery, IEEE Transactions on*, vol. 15, no. 2, pp. 665–669, Apr 2000.

[18] T. H. Cormen, C. E. Leiserson, and R. L. Rivest, *Introducion to Algorithms*. Mc Graw Hill, 1990.

[19] Z. Ding, S. Srivastava, and D. Cartes, "Expert system based dynamic load shedding scheme for shipboard power systems," *Industry Applications Conference, 2006. 41st IAS Annual Meeting. Conference Record of the 2006 IEEE*, vol. 3, pp. 1338–1344, Oct. 2006.

[20] N. Doerry, "Zonal ship design." *American Society of Naval Engineers. Naval Engineers Journal*, vol. 118(1), pp. 39–53, 2006.

[21] W. G. E. Solodovnik and R. Dougal, "Zonal ship power system." *Naval Engineers Journal*, vol. 114, 2002.

[22] A. Estremera, *Design of a Reconfiguration Controller for a DC Zonal Distribution System*. M.S. Thesis. University of Puerto Rico, Mayagüez, 2005.

[23] J.-Y. Fan, L. Zhang, and J. McDonald, "Distribution network reconfiguration: single loop optimization," *Power Systems, IEEE Transactions on*, vol. 11, no. 3, pp. 1643–1647, Aug 1996.

[24] A. Feliachi, K. Schoder, S. Ganesh, and H.-J. Lai, "Distributed control agents approach to energy management in electric shipboard power system," *Power Engineering Society General Meeting, 2006. IEEE*, pp. 6 pp.–, June 2006.

[25] A. Flueck and Z. Li, "Destination: Perfection," *Power and Energy Magazine, IEEE*, vol. 6, no. 6, pp. 36–47, November-December 2008.

[26] S. Ghosh and D. Das, "Method for load-flow solution of radial distribution networks," *Generation, Transmission and Distribution, IEE Proceedings-*, vol. 146, no. 6, pp. 641–648, Nov 1999.

[27] S. Ghosh, A. Gupta, and S. V. Pemmaraju, "A self-stabilizing algorithm for the maximum flow problem," *Distrib. Comput.*, vol. 10, no. 4, pp. 167–180, 1997.

[28] A. V. Goldberg and R. E. Tarjan, "A new approach to the maximum-flow problem," *J. ACM*, vol. 35, no. 4, pp. 921–940, 1988.

[29] J. G. Gómez-Gualdrón., *A Multiagent System Approah for a Self-reconfigurable Electric Power Distribution System.* M.S. Thesis University of Puerto Rico, Mayagüez, 2005.

[30] Y.-T. Hsiao, "Multiobjective evolution programming method for feeder reconfiguration," *Power Systems, IEEE Transactions on*, vol. 19, no. 1, pp. 594–599, Feb. 2004.

[31] Y. Huang, *Fast Reconfiguration Algortihm Development for Shipboard Power Systems.* M.S. Thesis Mississippi State University, 2005.

[32] S. K. J. Momoh and W. Salawu, "Security assessment of dc zonal naval-ship power system," in *Large Engineering Systems Conference on Power Engineering*, 2001.

[33] I. Jonasson and L. Soder, "Power quality on ships. a questionnaire evaluation concerning island power system," *Harmonics and Quality of Power, 2000. Proceedings. Ninth International Conference on*, vol. 2, pp. 639–644 vol.2, 2000.

[34] L. F. Jr and D. R. Fulkerson, *Flows in Network.* Princeton, 1962.

[35] S. Khushalani and N. Schulz, "Restoration optimization with distributed generation considering islanding," *Power Engineering Society General Meeting, 2005. IEEE*, pp. 2445–2449 Vol. 3, 12-16 June 2005.

[36] P. Kundur, *Power System Stability and Control.* McGraw-Hill, Inc., 1993.

[37] I. J. V. Laurens, "A decentralized negotiation framework for restoring electrical energy delivery networks with intelligent power routers - iprs," Master's thesis, University of Puerto Rico, Mayagez Campus, 2005.

[38] S. Lee and J. Grainger, "Evaluation of the applicability of the network flow approach to the emergency service restoration problem," *Circuits and Systems, 1988., IEEE International Symposium on*, pp. 909–912 vol.1, 7-9 Jun 1988.

[39] W.-M. Lin and H.-C. Chin, "A new approach for distribution feeder reconfiguration for loss reduction and service restoration," *Power Delivery, IEEE Transactions on*, vol. 13, no. 3, pp. 870–875, Jul 1998.

[40] K. Logan, "Intelligent diagnostic requirements of future all-electric ship integrated power system," *Petroleum and Chemical Industry Conference, 2005. Industry Applications Society 52nd Annual*, pp. 151–163, Sept. 2005.

[41] D. Luenberger, *linear and nonlinear programming.* addison wesley, 1984.

[42] N. Mahajan and M. Baran, "System reconfiguration on shipboard dc zonal electrical system," *Electric Ship Technologies Symposium, 2005 IEEE*, pp. 86–92, 25-27 July 2005.

[43] K. N. Miu and H.-D. Chiang, "Service restoration for unbalanced radial distribution systems with varying loads: solution algorithm," *Power Engineering Society Summer Meeting, 1999. IEEE*, vol. 1, pp. 254–258 vol.1, 18-22 Jul 1999.

[44] K. Miu, H.-D. Chiang, B. Yuan, and G. Darling, "Fast service restoration for large-scale distribution systems with priority customers and constraints," *Power Systems, IEEE Transactions on*, vol. 13, no. 3, pp. 789–795, Aug 1998.

[45] A. Morton and I. Mareels, "An efficient brute-force solution to the network reconfiguration problem," *Power Delivery, IEEE Transactions on*, vol. 15, no. 3, pp. 996–1000, Jul 2000.

[46] A. Morton and J. Mareels, "Overload prevention and loss minimization in managed distribution networks," *Power Delivery, IEEE Transactions on*, vol. 15, no. 3, pp. 972–977, Jul 2000.

[47] A. B. Morton, *Managed DC Power Reticulation Systems.* Ph.D Thesis University of Melbourne, Australia, 1999.

[48] K. Nagaraj, J. Carroll, T. Rosenwinkel, A. Arapostathis, M. Grady, and E. Powers, "Perspectives on power system reconfiguration for shipboard applications," *Electric Ship Technologies Symposium, 2007. ESTS '07. IEEE*, pp. 188–195, 21-23 May 2007.

[49] T. Nagata and H. Sasaki, "A multi-agent approach to power system restoration," *Power Systems , IEEE Transactions on*, vol. 17, no 2, pp. 457–462, May 2002.

[50] K. Nara, A. Shiose, M. Kitagawa, and T. Ishihara, "Implementation of genetic algorithm for distribution systems loss minimum re-configuration," *Power Systems, IEEE Transactions on*, vol. 7, no. 3, pp. 1044–1051, Aug 1992.

[51] A. Ouroua, L. Domaschk, and J. Beno, "Electric ship power system integration analyses through modeling and simulation," *Electric Ship Technologies Symposium, 2005 IEEE*, pp. 70–74, 25-27 July 2005.

[52] C. Petry and J. Rumburg, "Zonal electrical distribution systems: An affordable architecture for the future." *Naval Engineers Journal*, vol. 105, pp. 45–51, May 1993.

[53] B.-L. Qin, A. Guzman-Casillas, and I. Schweitzer, E.O., "A new method for protection zone selection in microprocessor-based bus relays," *Power Delivery, IEEE Transactions on*, vol. 15, no. 3, pp. 876–887, Jul 2000.

[54] T. L. M. R. K. Ahuja and J.B.Orlin, *Network Flows*. Prentice Hall, 1993.

[55] B. Radha, R. Ah King, and H. Rughooputh, "Optimal network reconfiguration of electrical distribution systems," *Industrial Technology, 2003 IEEE International Conference on*, vol. 1, pp. 66–71 Vol.1, 10-12 Dec. 2003.

[56] E. Ramos, J. Martinez-Ramos, A. Exposito, and A. Salado, "Optimal reconfiguration of distribution networks for power loss reduction," *Power Tech Proceedings, 2001 IEEE Porto*, vol. 3, pp. 5 pp. vol.3–, 2001.

[57] P. Rao and K. Rao, "An efficient load shedding algorithm for radial systems," *TENCON 2003. Conference on Convergent Technologies for Asia-Pacific Region*, vol. 2, pp. 771–774 Vol.2, 15-17 Oct. 2003.

[58] C. M. Roney-Dougal, *Graph Theory.* University of St Andrews, School of Mathematics and Statistics, 2007.

[59] N. Sarma, S. Ghosh, K. Prakasa Rao, and M. Srinivas, "Real time service restoration in distribution networks-a practical approach," *Power Delivery, IEEE Transactions on*, vol. 9, no. 4, pp. 2064–2070, Oct 1994.

[60] D. Shirmohammadi and H. Hong, "Reconfiguration of electric distribution networks for resistive line losses reduction," *Power Delivery, IEEE Transactions on*, vol. 4, no. 2, pp. 1492–1498, Apr 1989.

[61] S. Srivastava, K. Butler-Purry, and N. Sarma, "Shipboard power restored for active duty," *Computer Applications in Power, IEEE*, vol. 15, no. 3, pp. 16–23, Jul 2002.

[62] A. Stankovic and M. Calovic, "Graph oriented algorithm for the steady-state security enhancement in distribution networks," *Power Delivery, IEEE Transactions on*, vol. 4, no. 1, pp. 539–544, Jan 1989.

[63] C.-L. Su and C.-T. Yeh, "Probabilistic security analysis of shipboard dc zonal electrical distribution systems," *Power and Energy Society General Meeting - Conversion and Delivery of Electrical Energy in the 21st Century, 2008 IEEE*, pp. 1–7, July 2008.

[64] NSF/ONR Electric Power Networks Efficiency and `Security` (EPNES), "ONR control challenge problem," *Available: http://www.usna.edu/EPNES.*, January 2002.

[65] T. Thakur and Jaswanti, "Study and characterization of power distribution network reconfiguration," *Transmission & Distribution Conference and Exposition: Latin America, 2006. TDC '06. IEEE/PES*, pp. 1–6, Aug. 2006.

[66] P. Tulpule, K. Schoder, A. Feliachi, and H.-J. Lai, "Distributed approaches for determination of reconfiguration algorithm termination," *Electric Ship Technologies Symposium, 2007. ESTS '07. IEEE*, pp. 169–174, 21-23 May 2007.

[67] J. Wan and K. Nan Miu, "A zonal-load estimation method for unbalanced, radial distribution networks," *Power Delivery, IEEE Transactions on*, vol. 17, no. 4, pp. 1106–1112, Oct 2002.

[68] P. Wang, "Linear graphs and modification methods for network matrices," *Circuits and Systems, 1991., IEEE International Sympoisum on*, pp. 1002–1004 vol.2, 11-14 Jun 1991.

[69] O. Wasynczuk, E. Walters, and H. Hegner, "Simulation of a zonal electric distribution system for shipboard applications," *Energy Conversion Engineering Conference, 1997. IECEC-97., Proceedings of the 32nd Intersociety*, vol. 1, pp. 268–273 vol.1, 27 Jul-1 Aug 1997.

[70] P. Yan and A. Sekar, "Analysis of radial distribution systems with embedded series facts devices using a fast line flow-based algorithm," *Power Systems, IEEE Transactions on*, vol. 20, no. 4, pp. 1775–1782, Nov. 2005.